

# Global Biogeochemical Cycles<sup>®</sup>

## RESEARCH ARTICLE

10.1029/2024GB008201

### Key Points:

- Compound extreme-events (e.g., hot + dry extreme-events) cause large impacts on daily CH<sub>4</sub> emissions relative to discrete extreme-events
- Dry-only extreme-events show large total decreases in CH<sub>4</sub> emissions due to the long duration of events, despite initial flux increases
- Lagged impacts are significant for at least the 12 months following most types of extreme-events

### Supporting Information:

Supporting Information may be found in the online version of this article.

### Correspondence to:

T. J. R. Lippmann,  
t.j.r.lippmann@vu.nl

### Citation:

Lippmann, T. J. R., van der Velde, Y., Naudts, K., Hensgens, G., Vonk, J. E., & Dolman, H. (2024). Simultaneous hot and dry extreme-events increase wetland methane emissions: An assessment of compound extreme-event impacts using Ameriflux and FLUXNET-CH<sub>4</sub> site data sets. *Global Biogeochemical Cycles*, 38, e2024GB008201. <https://doi.org/10.1029/2024GB008201>

Received 17 APR 2024

Accepted 29 AUG 2024

### Author Contributions:

**Conceptualization:** T. J. R. Lippmann  
**Data curation:** T. J. R. Lippmann  
**Formal analysis:** T. J. R. Lippmann  
**Supervision:** Y. van der Velde, K. Naudts, J. E. Vonk  
**Writing – original draft:** T. J. R. Lippmann  
**Writing – review & editing:** T. J. R. Lippmann, Y. van der Velde, K. Naudts, G. Hensgens, J. E. Vonk, H. Dolman

© 2024 The Author(s).

This is an open access article under the terms of the [Creative Commons Attribution-NonCommercial License](#), which permits use, distribution and reproduction in any medium, provided the original work is properly cited and is not used for commercial purposes.

## Simultaneous Hot and Dry Extreme-Events Increase Wetland Methane Emissions: An Assessment of Compound Extreme-Event Impacts Using Ameriflux and FLUXNET-CH<sub>4</sub> Site Data Sets

T. J. R. Lippmann<sup>1</sup> , Y. van der Velde<sup>1</sup>, K. Naudts<sup>1</sup>, G. Hensgens<sup>1</sup> , J. E. Vonk<sup>1</sup>, and H. Dolman<sup>1,2</sup>

<sup>1</sup>Vrije Universiteit Amsterdam, Amsterdam, The Netherlands, <sup>2</sup>Royal Netherlands Institute for Sea Research, Texel, The Netherlands

**Abstract** Wetlands are the largest natural source of global atmospheric methane (CH<sub>4</sub>). Despite advances to our understanding of changes in temperature and precipitation extremes, their impacts on carbon-rich ecosystems such as wetlands, remain significantly understudied. Here, we quantify the impacts of extreme temperature, precipitation, and dry events on wetland CH<sub>4</sub> dynamics by investigating the effects of both compound and discrete extreme-events. We use long-term climate data to identify extreme-events and 45 eddy covariance sites data sets sourced from the FLUXNET-CH<sub>4</sub> database and Ameriflux project to assess impacts on wetland CH<sub>4</sub> emissions. These findings reveal that compound hot + dry extreme-events lead to large increases in daily CH<sub>4</sub> emissions. However, per event, discrete dry-only extreme-events cause the largest total decrease in CH<sub>4</sub> emissions, due to their long duration. Despite dry-only extreme-events leading to an overall reduction in CH<sub>4</sub> emissions, enhanced fluxes are often observed for the first days of dry-only extreme-events. These effects differ depending on wetland type, where marsh sites tend to be sensitive to most types of extreme-events. Lagged impacts are significant for at least the 12 months following several types of extreme-events. These findings have implications for understanding how extreme-event impacts may evolve in the context of climate change, where changes in the frequency and intensity of temperature and precipitation extreme-events are already observed. With increasing occurrences of enhanced CH<sub>4</sub> fluxes in response to hot-only extreme-events and hot + wet extreme-events and fewer occurrences of reduced CH<sub>4</sub> fluxes during cold-only extreme-events, the impact of wetland CH<sub>4</sub> emissions on climate warming may be increasing.

## 1. Introduction

Wetlands are the largest natural source of global atmospheric methane (CH<sub>4</sub>), with natural sources (wetlands and inland waterbodies) contributing approximately 50% of total global CH<sub>4</sub> emissions (Saunio et al., 2020), whilst providing a large array of regulating, sustaining and cultural services (Harrison et al., 2010). Wetlands have played a pivotal role driving significant fluctuations in global CH<sub>4</sub> emissions in recent decades (Nisbet et al., 2023; Peng et al., 2022), and are projected to play an increasing role driving 21st century warming (Zhang et al., 2017). Extreme climate events, such as heat waves and droughts are increasing in both frequency and intensity due to human-induced climate change (Intergovernmental Panel on Climate Change (IPCC), 2023). Observations show that heavy precipitation extreme-events are occurring more frequently and with greater intensity (Du et al., 2019). Extreme climate events directly impact ecosystem functioning (Reichstein et al., 2013) and land surface properties (e.g., soil moisture), creating positive and negative feedbacks with the atmosphere (Seneviratne et al., 2006, 2012). Discrete (or univariate) extreme-events are events where a single variable is in an extreme state whereas compound extreme-events involve two or more drivers (such as simultaneous extreme heat and drought) and can lead to severe ecosystem impacts (Leonard et al., 2014; Seneviratne et al., 2012).

Carbon dioxide fluxes have for a long time been used as the indicator for ecosystem net carbon gain or loss (Schwalm et al., 2012; Wolf et al., 2016). However, research has shown that carbon loss via CH<sub>4</sub> fluxes have an equally important role on warming, relative to CO<sub>2</sub> fluxes (Zhuang et al., 2015; Zou et al., 2022). Compared to our understanding of the impacts of extreme-events on CO<sub>2</sub> fluxes (Von Buttlar et al., 2018; Zscheischler et al., 2014), we know relatively little as to how CH<sub>4</sub> emissions at the ecosystem level respond to extreme-events (Zhang et al., 2017). Previous multi-site syntheses that have assessed the impacts of extreme climate events on

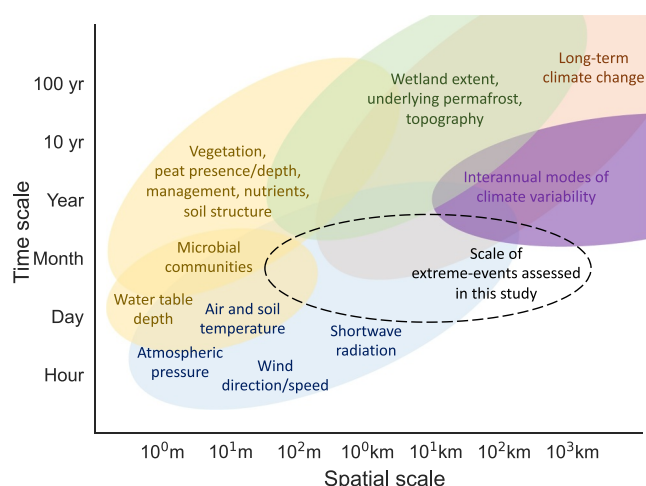


**Figure 1.** Wetland  $\text{CH}_4$  emissions are the result of local site characteristics, which are in turn affected by regional-scale systems, which are in turn impacted by planetary-scale features. Schematic identifying the characteristic processes driving wetland  $\text{CH}_4$  emissions, and their relevant spatial and temporal scales. Included are driving processes that are limited to local impacts (blue), microtopography and site properties (gold), which overlap with regional driving processes, such as permafrost presence (green), as well as large scale processes, such as interannual modes of climate variability (purple) and long-term climate change (orange). The black dashed line outlines the scales relevant for the extreme-events assessed in this study.

ecosystems GHG emissions have been largely limited to investigating the impacts on  $\text{CO}_2$  fluxes (Bastos, O'Sullivan et al., 2020; Zscheischler et al., 2013, 2014).

Extreme event impacts on wetlands are the result of local site characteristics and local-scale extreme-event occurrence and intensity, which are in turn affected by larger-scale systems (e.g., location of the jet stream), which are in turn impacted by planetary-scale features such as shifts in the radiation balance (Figure 1). The relative strength of each of these drivers varies between sites, and is also dependent on the time scale considered (e.g., diurnal vs. seasonal vs. centennial) (Knox et al., 2021; Treat et al., 2018). Surface  $\text{CH}_4$  emissions are the outcome of belowground  $\text{CH}_4$  production, oxidation and the transport of  $\text{CH}_4$  from below-to aboveground (Vroom et al., 2022). On daily and seasonal time scales, soil and air temperatures have been found to be dominant drivers of  $\text{CH}_4$  flux variability, however, water levels and vegetation composition also play important roles (Long et al., 2010; Sturtevant et al., 2016). Significant changes to wetland extent (Zhuang et al., 2015), artificial drainage or rewetting have the potential to override these dynamics (Zou et al., 2022). Simultaneous changes to temperature and water levels lead to interacting responses where, higher  $\text{CH}_4$  emissions have been observed in plots subjected to both warming and flooding (raised water table) (Turetsky et al., 2008).

Significant impacts to wetland ecosystems have been documented during and following heat waves, droughts, and other extreme-events. The heatwave caused by the European summer 2003 climate anomaly caused substantial die-off of Sphagnum moss, the primary plant responsible for peat develop-

ment and carbon accumulation in peatlands, with sustained impacts for at least the 4 subsequent years across 20 Alpine bogs (Bragazza, 2008). The warm and dry conditions of the 2018 European drought led to a lowering of the water table at several mire sites leading to reduced  $\text{CH}_4$  emissions (Rinne et al., 2020). A series of drought experiments in a range of wetland systems, observed reduced  $\text{CH}_4$  emissions due to enhanced methanotrophic oxidation under drier conditions (Borken et al., 2006; Davidson et al., 2008; Olefeldt et al., 2017), where, reduced emissions have continued beyond the length of the drought (Kang et al., 2018). However, an experimental drought study saw an initial release of  $\text{CH}_4$ , followed by reduced emissions, persisting beyond the drought itself (Dowrick et al., 2006).

Lagged ecosystem responses encompass complex overlapping, asynchronous responses to environmental change (Ruehr et al., 2019; Seneviratne et al., 2012). In particular drought, or extended dry periods, have lasting ecosystem consequences (Frank et al., 2015). During extreme-events, plants may change their quality, quantity and timing of litter and rhizodeposition, impacting SOM fractions leading to shifts in microbial populations, and therefore  $\text{CH}_4$  emissions (Nazaries et al., 2013; Reichstein et al., 2013). Field studies monitoring the impacts of extended dry periods on vegetation and  $\text{CH}_4$  emissions have reported vegetation die-off during drought accompanied by reduced emissions, followed by the establishment of introduced species during rewetting, and enhanced emissions following rewetting (Kosten et al., 2018; Malone et al., 2013). Methane production by methanogenesis has recovered quickly after rewetting following drought, however, positive  $\text{CH}_4$  fluxes to the atmosphere (indicative of replenished soil  $\text{CH}_4$  concentrations) were delayed (Knorr & Blodau, 2009; Olefeldt et al., 2017). In a long-term experimental study investigating the impacts of intensified winter soil frost, reduced sedge leaf area and enhanced Sphagnum moss growth led to reduced  $\text{CH}_4$  emissions during subsequent growing seasons, and thereby reduced annual  $\text{CH}_4$  budgets (Zhao et al., 2016). Lagged and legacy effects of climate extreme-events are understood to significantly alter various components of the terrestrial carbon cycle (Reichstein et al., 2013).

The changing intensity and frequency of temperature and precipitation extremes, alongside ecosystem sensitivity and risk, varies seasonally and differs across regions (Seneviratne et al., 2012). Wetland extreme-event impacts are seasonally dependent, partly because wetland  $\text{CH}_4$  production shows enhanced temperature sensitivity during summer months (Li et al., 2023). High latitude carbon-rich ecosystems, such as permafrost and tundra

ecosystems, are at particular risk because conversion of a small fraction of these carbon pools into CH<sub>4</sub> can rapidly increase the rate of future climate change (Christensen et al., 2021; Schuur et al., 2015).

Eddy covariance (EC) measurements can be used to provide an estimate of the ecosystem-scale response to changing climate or environment. The FLUXNET-CH<sub>4</sub> data set (Delwiche et al., 2021; Knox et al., 2019) and the Ameriflux project (Novick et al., 2018) provide measurements of the exchange of carbon (CH<sub>4</sub>, CO<sub>2</sub>), energy, and water between the land and the atmosphere. Here, we use 45 site data sets to study the effects of extreme temperature and precipitation events on CH<sub>4</sub> fluxes. Using these site data sets, we aim to (a) investigate the differences between compound (simultaneous) and discrete (univariate) extreme-events, (b) assess the cumulative impacts over the duration of extreme-events, (c) analyze the lagged impacts that extend beyond the length of the event itself, and (d) assess the effects of seasonality and wetland classification on CH<sub>4</sub> flux anomalies during extreme-events. We expect (a) compound extreme-events to generally lead to larger impacts than discrete extreme-events, (b) impacts increase with event duration, (c) wetland CH<sub>4</sub> emissions to return to baseline within days to weeks after the end of an extreme-event, and (d) the largest impacts will occur during warm months due to enhanced microbial temperature sensitivity, with differences between wetland types due to differences in physical properties like pH, soil and vegetation type.

## 2. Methods

To identify extreme-events over sufficiently long and consistent time periods for all sites, we used gridded climate data because the length of meteorological site measurements was insufficient for the long time periods required for extreme-event detection. Using the FLUXNET-CH<sub>4</sub> database and the Ameriflux project, we compared fluxes during these extreme-events with fluxes measured at the same time of the year, for other years, outside of extreme-events.

### 2.1. Extreme-Event Detection and Identification

Here, we explain the process used to identify discrete (univariate) extreme-events and compound (simultaneous) temperature and wet/dry extreme-events. Long-term daily temperature and precipitation data were used to identify extreme climate events. To identify extreme precipitation events, we used the gauge-based daily precipitation data set, GPCC Full Data Daily Version 2022 (GPCC), which is available for the period from January 1982 to December 2020 (Schamm et al., 2014; Ziese et al., 2018). To identify temperature extreme-events, we used the 5th generation ECMWF atmospheric reanalysis product for the land (ERA5-Land) over the same time period (Muñoz-Sabater et al., 2021). Extreme temperature, precipitation, and dry events were calculated for the period from January 1982 to December 2020.

An extreme event can occur in any season and therefore the daily time series were deseasonalized by subtracting the daily average of all years of data (Von Buttler et al., 2018). To do this the mean air temperature or precipitation for each day of the year was calculated across all available years. This was then smoothed with a 2 weeks moving average during a given year (Equation 1) and finally subtracted from the air temperature time series (Equation 2).

$$T_{ref}(t) = \frac{1}{Nn \cdot Ny} \sum_{n=-7}^7 \sum_{y=1982}^{2020} T(J(t+n, y)) \quad (1)$$

$$\Delta T(t) = T(t) - T_{ref}(t) \quad (2)$$

where,  $T(t)$  represents the daily air temperature or precipitation,  $J(t, y)$  represents the day of year at time,  $t$ , but in year,  $y$ .  $\Delta T$  denotes the climate anomaly,  $Nn$  is the number of days of the moving window and  $Ny$  is the number of years used to calculate the average temperature (or rainfall). A percentile-based approach (Seneviratne et al., 2012; Zscheischler et al., 2014) was used to define the upper and lower 5th percentile of the deseasonalized temperature distribution as extreme. To identify wet extreme-events, the upper 5th percentile of the deseasonalized precipitation distribution was defined as extreme (using Equation 1 and Equation 2). Tests using deseasonalized and non-deseasonalized precipitation data yielded consistent results. To identify extreme dryness, dry days were identified as days where total daily rainfall was <1 mm. Successive dry days were concatenated and the upper 10th percentile of the duration of consecutive dry days (CDD) were defined as dry extreme-events for each station. The 10th percentile was used in the calculation of dry extreme-events so that the number of all-dry

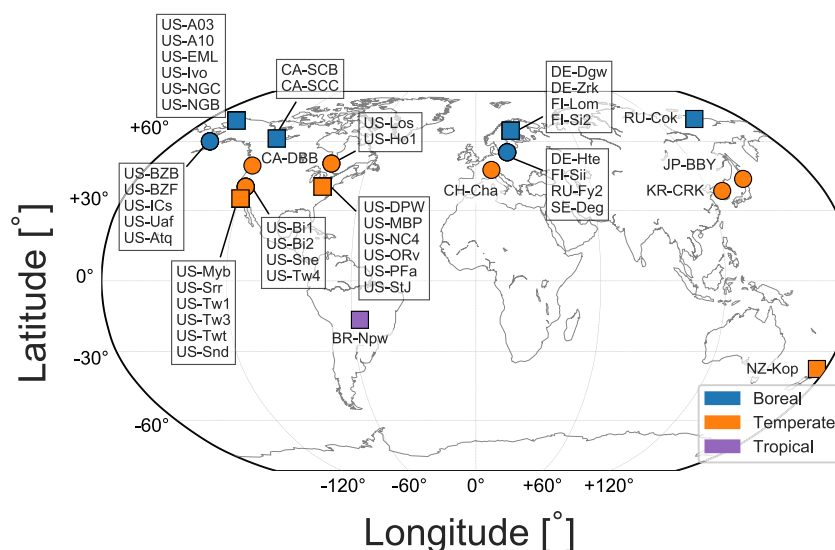


**Figure 2.** Geographical distribution of sites used in this study. Circular symbols represent sites included in all analyses in this study, while square symbols indicate sites limited to the assessment of temperature extreme-event impacts. This map was created using Matplotlib Basemap (<https://matplotlib.org/basemap/>).

extreme days was similar to the number of all-wet, all-cold, and all-hot extreme days. For the purposes of identifying extreme dry periods, it was not possible to deseasonalize the precipitation data. Nevertheless, the impacts of extreme dry periods on wetland  $\text{CH}_4$  fluxes may be seasonally dependent and therefore the seasonal impacts of extreme dry periods on  $\text{CH}_4$  fluxes were assessed.

To differentiate between the effects of discrete (univariate) extreme-events and compound (simultaneous) temperature and wet/dry extreme-events, the following types of extreme-events were distinguished (Table S1 in Supporting Information S1): (a) extreme-events irrespective of possible simultaneous extreme-events (i.e., all-hot, all-cold, all-wet, and all-dry), (b) discrete extreme-events (i.e., hot-only, cold-only, wet-only, dry-only) and (c) compound extreme-events (i.e., hot + dry, hot + wet, cold + wet, cold + dry). Compound extreme-events were identified as multiple extreme-events occurring simultaneously on a given day. Discrete extreme-events were identified as only a single extreme-event occurring on a given day. Additionally, if the period between two consecutive extreme-events was shorter than 20% of the combined length of the two extreme-events together, the two successive extreme-events were treated as one single event (Von Buttlar et al., 2018).

## 2.2. Flux and Site Data Selection

We used site-based EC flux tower data sets with more than 3 years of flux measurements available under the CC-BY-4.0 data use policy from the Ameriflux project (Novick et al., 2018) and the FLUXNET- $\text{CH}_4$  initiative (Delwiche et al., 2021; Knox et al., 2019). Of the 577 sites in the Ameriflux project under the CC-BY-4.0 data use policy, 123 sites measured  $\text{CH}_4$  fluxes, and 45 sites had  $\text{CH}_4$  flux measurement records spanning at least 3 years. Of the 81 sites in the FLUXNET- $\text{CH}_4$  database, 37 sites had  $\text{CH}_4$  flux measurement records spanning at least 3 years. The urban wetland site, UK-LBT, was omitted along with lake site, DE-Dgw, because these sites capture  $\text{CH}_4$  emission processes outside the scope of this study. To determine which sites could be included in the assessment of both precipitation and temperature extreme-events, correlations of both temperature and precipitation long-term gridded climate data and site-based data were calculated using a simple linear regression model. If the  $R^2$  value was less than 0.9, for either temperature or precipitation, the time series of the grid box with an  $R^2$  closest to 1.0 from the nine nearest grid boxes (i.e., the direct neighboring pixels to the grid box with the EC tower) was tested. Stations with an  $R^2 < 0.6$  were omitted from the study. This resulted in 45 sites being selected for inclusion in the assessment of temperature extreme-events and 20 sites in the assessment of dry extreme-events, precipitation extreme-events, compound extreme-events, and discrete extreme-events (Table S2 in Supporting Information S1, Figure 2).

All sites included in this study are representative of a wet system and were classified by wetland type - including bog ( $n = 8$ ), fen ( $n = 10$ ), drained ( $n = 4$ ), upland ( $n = 6$ ), marsh ( $n = 6$ ), rice ( $n = 2$ ), and wet tundra ( $n = 8$ ). The two salt marsh sites were excluded from the wetland classification analysis due to a lack of data. Wetlands were classified according to the FLUXNET-CH<sub>4</sub> metadata (using the “SITE\_CLASSIFICATION” variable) and site literature.

Variable, “FCH<sub>4</sub>” was used to assess CH<sub>4</sub> fluxes. From the FLUXNET-CH<sub>4</sub> data set, non-gap-filled aggregated daily flux measurements were used and gap-filled data was included only if the time between two actual measurements was 24 hr, and otherwise excluded. For site data accessed through Ameriflux, half hourly measurements were aggregated to daily averages if more than 70% of original measurements or high confidence gap-filled (QC flag “0”) data were available and was only included if the time between two actual measurements was less than 24 hr. Tests comparing our aggregated data and entirely non-gap-filled data confirmed that our conclusions remained consistent. For tall towers, the storage correction term, “SCH<sub>4</sub>,” was added to CH<sub>4</sub> flux measurements. We did not exclude data based on the length of data gaps because some sites included in this study lie within the Arctic where measurements are only available for the growing season but at times, for several consecutive years. Instead, daily flux data was included where at least 3 years of data were available for that day of the year, and otherwise excluded.

Differences in CH<sub>4</sub> flux sensitivity across sites may impede a straightforward assessment of extreme-event impacts and therefore each site flux data set was normalized by standard deviation (Equation 3). Analyses were completed using both normalized and native CH<sub>4</sub> flux units and our conclusions remain consistent for both normalized and non-normalized data. This manuscript presents CH<sub>4</sub> flux anomalies calculated using normalized site fluxes [–].

$$z(t) = \frac{f(t) - \bar{f}}{\sigma(f)} \quad (3)$$

where,  $f$  represents the daily flux  $\bar{f}$  represents the mean of daily site fluxes,  $\sigma(f)$  represents the standard deviation of the daily site fluxes, and  $z$  [–] denotes the normalized daily flux.

For each extreme-event day, the daily flux anomaly was defined as the difference between the mean daily flux and a comparable reference period (Equation 5), calculated using normalized fluxes. The reference period was defined as the mean of the day of the year for all other years with available site data and then smoothed using a 14 days moving-average (Equation 4). Anomalies are therefore only representative of extreme-event days with available measurements.

$$z_{ref}(t) = \frac{1}{Nn \cdot Ny} \sum_{n=-7}^7 \sum_{y=1982}^{2020} z(J(t+n, y)) \quad (4)$$

$$\Delta Z(t) = z(t) - z_{ref}(t) \quad (5)$$

where,  $\Delta Z$  represents the normalized flux anomaly. Tests using a 7 and 21 days moving-average confirmed that our conclusions remain consistent when calculated relative to both shorter and longer moving-average windows (Figure S1 in Supporting Information S1).

One complication when estimating the impacts of wet extreme-events on CH<sub>4</sub> flux measurements is that EC towers have difficulty to measure during moments of heavy precipitation because the open-path instrumentation (e.g., sonic anemometers) are affected by water droplets (Burns et al., 2015). On rainy days, the intermittent, often start, stop, nature of precipitation means that flux measurements may be possible during rain-free moments. To maintain high quality flux data, we have restricted the analysis to only include data if more than 70% of original measurements or high confidence gap-filled data were available, only using high quality gap filled data if the time between two actual measurements was 24 hr or less.



### 2.3. Assessment of Extreme-Event Impacts on CH<sub>4</sub> Fluxes

We first assessed the impacts of extreme-events that occurred irrespective of other simultaneous extreme-events (all-hot, all-cold, all-wet, all-dry) on wetland CH<sub>4</sub> emissions. We then compared the impacts of compound extreme-events (cold + dry, hot + dry, hot + wet, cold + wet), discrete extreme-events (cold-only, hot-only, wet-only, and dry-only), against extreme-events that occurred irrespective of other simultaneous extreme-events (all-hot, all-cold, all-wet, all-dry) on wetland CH<sub>4</sub> emissions.

To understand the ecosystem response to both compound and discrete extreme-events, we assessed three types of responses: (a) CH<sub>4</sub> flux anomalies during the event; (b) cumulative CH<sub>4</sub> flux anomalies over the event duration; (c) CH<sub>4</sub> flux anomalies extending beyond the length of the extreme-event itself (lagged response). To test for statistical significance, flux anomalies were compared against reference data where the reference data consisted of all flux data, excluding extreme-events. The lagged response was evaluated by comparing the daily CH<sub>4</sub> flux anomalies for the 12 month period after the event against the CH<sub>4</sub> flux anomalies during reference years. The reference data for this analysis excluded the year following the event as well as other extreme-events.

We quantified the ecosystem response to both compound and discrete extreme-events using the entire data set, but also assessed the role of (a) seasonality (northern hemisphere summer, spring, winter, and autumn), and (b) wetland classification. These assessments were limited to the northern hemisphere because the two southern hemisphere sites did not qualify for inclusion in the compound and discrete extreme-events assessment due to poor correlation between site precipitation data and the long-term GPCC precipitation record.

The sign convention in this paper is that a positive gas flux is indicative of the flux entering the atmosphere and therefore, a positive flux anomaly indicates a higher than average emission. To test for statistical significance, the Mann-Whitney U test was used to compare distributions and the Welch's *t*-test was used to specifically compare the mean of distributions. The Mann-Whitney U test is a nonparametric test that determines if it possible to reject the null hypothesis that both samples come from the same population, without making the assumption that the two populations are normally distributed. The Welch's *t*-test is a two-sample location test, suitable for populations with unequal variances and sample size, to test if two populations have equal means. All analyses were conducted using Python three and the statistical tests were performed using the SciPy and pyMannKendall Python packages.

### 2.4. Changing Extreme-Event Frequency

To provide a picture of how extreme-events are changing at these wetland sites, we calculated linear trends using longterm climate data. We used the median of pairwise slopes method (or Sen's trend estimator) to calculate long-term trends (Aschrott, 2021; Sen, 1968), and trend significance was estimated using the Mann-Kendall test (Farlie & Kendall, 1971).

## 3. Results

Firstly, we assess the changing frequency of extreme-events at these wetland sites (Section 3.1). We then investigate the effects of extreme-events on wetlands by assessing the mean daily CH<sub>4</sub> flux anomalies (Section 3.2). Thirdly, we assess the changing and cumulative impacts over the duration of extreme-events (Section 3.3) and lastly, the lagged impacts (Section 3.4). All CH<sub>4</sub> flux anomalies are calculated using unitless [–] normalized daily site fluxes (Equation 3).

### 3.1. Changing Extreme-Event Frequency at Wetland Sites

Over the past decades, notable changes have occurred in the frequency and intensity of climate extreme-events at these wetland sites (Figure 3). Cold-only and hot-only extreme-events showed strong longterm trends where the decrease in the frequency of cold-only extreme-events ( $-7.7 \text{ days year}^{-1}$ ) was larger than the increase in hot-only extreme-events ( $5.4 \text{ days year}^{-1}$ , Figure 3). Discrete extreme-events occurred more often than compound extreme-events, over the entire assessment period. There was no significant change in the frequency of most compound extreme-events (cold + dry, cold + wet, hot + dry), although a slight positive trend in the frequency of hot + wet extreme-events ( $+0.2 \text{ days year}^{-1}$ ) was observed.

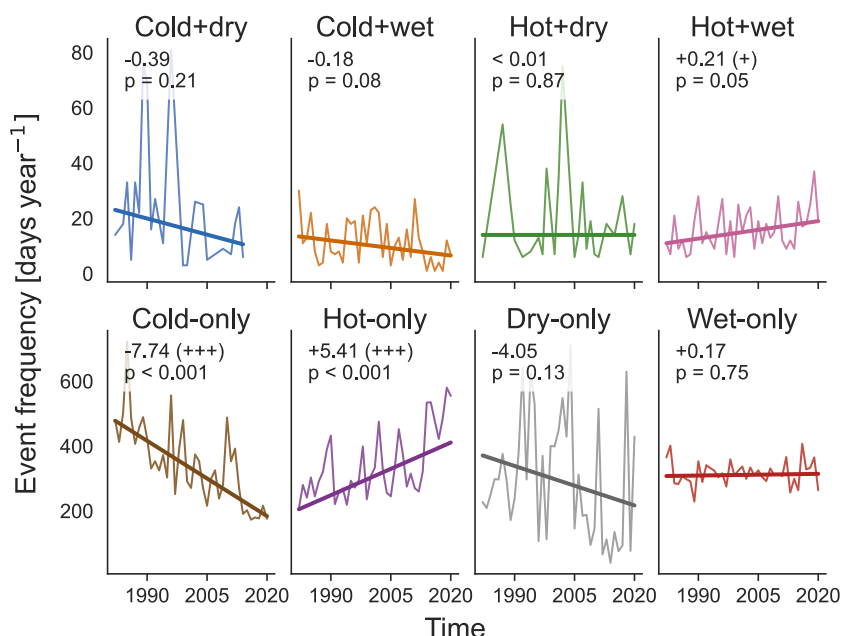


**Figure 3.** Extreme-event frequency is changing at these wetland sites. Average trends (days per year) of extreme-event occurrence across all sites and the associated statistical significance (p). Statistically significant trends are indicated by: +++ (p < 0.001), ++ (p < 0.01), + (p < 0.05). Note the different y axes.

### 3.1.1. Increasing Hot-Only Extreme-Event Frequency Across all Seasons

Seasonal results showed significant warming in all seasons (Figure S5 in Supplementary Information S1). The largest changes have occurred during spring hot-only extreme-events (2.0 days year<sup>-1</sup>), autumn cold-only extreme-events (−5.3 days year<sup>-1</sup>), and spring dry-only extreme-events (−2.9 days year<sup>-1</sup>). Strong decreases in the frequency of cold-only extreme-events were observed during winter (−2.9 days year<sup>-1</sup>) and summer (−0.5 days year<sup>-1</sup>) extreme-events. The changing frequency of hot-only extreme-events was observed across all other seasons - winter (1.6 days year<sup>-1</sup>), summer (1.1 days year<sup>-1</sup>), and autumn (1.0 days year<sup>-1</sup>). These results indicate several significant longterm trends in extreme-event frequency with substantial differences across seasons.

### 3.2. Compound Extreme-Events Impact CH<sub>4</sub> Flux Anomalies

Compound extreme-events (Figures 4a–4d) influenced both the magnitude and at times, the direction of CH<sub>4</sub> flux anomalies relative to the impacts of all-hot, all-cold, all-wet, all-dry extreme-events (Figures 4e–4h). Hot + dry extreme-events (1.11 ± 1.32) led to the largest flux anomalies, where impacts were significantly different to both all-dry and all-hot extreme-events (p < 0.05), and the reference data (p < 0.001). Cold + wet extreme-events (−0.34 ± 0.22) led to notably reduced CH<sub>4</sub> fluxes with low variability, significantly different to the impacts of all-wet and all-cold extreme-events (p < 0.05), and the reference data (p < 0.01). Hot + wet extreme-events (0.32 ± 0.86) caused notably enhanced CH<sub>4</sub> fluxes, significantly different (p < 0.05) to the reference data but not significant relative to the impacts of all-hot extreme-events or all-wet extreme-events. Hot-only extreme-events (0.21 ± 0.81) led to notably enhanced CH<sub>4</sub> fluxes, significantly different (p < 0.001) to the reference data but not significant relative to the impacts of all-hot extreme-events. Mean CH<sub>4</sub> flux anomalies during dry-only extreme-events (−0.03 ± 0.84) and wet-only extreme-events (0.05 ± 0.9) were minimal but highly variable. Flux anomalies were not observed during cold + dry extreme-events or cold-only extreme-events. It is important to note that compound extreme-events occurred less frequently than discrete extreme-events and therefore, the number of measurements were also less. For example, there were 1128 days of CH<sub>4</sub> flux measurements during hot-only extreme-events but only 53 days of measurements during hot + dry extreme-events. The distributions of compound and discrete extreme-events emphasize how strongly compound and discrete extreme-events differ from all-hot, all-cold, all-wet, all-dry extreme-events (Figure S3 in Supporting Information S1).

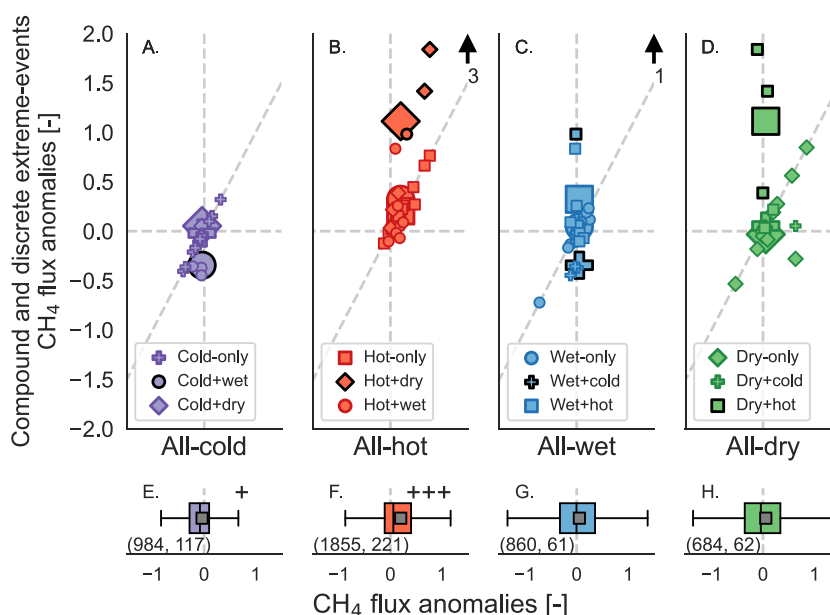


**Figure 4.** Compound extreme-events influence the magnitude and the direction of  $\text{CH}_4$  flux anomalies relative to the impacts of all-hot, all-cold, all-wet, all-dry events. (a–d) Flux anomalies during compound and discrete events (y axis) are plotted (and tested for statistical significance) against the impacts of all-cold, all-hot, all-wet and all-dry extreme-events (x axis). Statistical significance ( $p < 0.05$ ) is indicated using a black outline. Average anomalies across all sites are shown using large markers and individual sites are shown using small markers. Black arrows indicate data points outside the plot range. (d–f) Box plots show upper and lower quartile (boxes), median (black line), mean (gray square), smallest and largest values without outliers (whiskers). The number of data points and outliers are written in brackets along the x axis. Statistical significance relative to the reference data is indicated by: +++ ( $p < 0.001$ ), ++ ( $p < 0.01$ ), + ( $p < 0.05$ ).

Without checking whether extreme-events were compound or discrete in nature, extreme temperature-events (all-hot and all-cold) led to significant impacts, whereas all-wet and all-dry events did not (Figures 4e–4h). All-hot extreme-events ( $0.20 \pm 0.76$ , mean  $\pm$  standard deviation) generally caused enhanced  $\text{CH}_4$  flux anomalies, significantly different ( $p < 0.001$ ) to the reference data (Figure S3 in Supporting Information S1). Conversely, all-cold extreme-events ( $-0.04 \pm 0.61$ ) resulted in minimally reduced flux anomalies, significantly different to the reference data ( $p < 0.05$ ). Both all-dry extreme-events ( $0.05 \pm 0.93$ ) and all-wet extreme-events ( $0.05 \pm 0.9$ ) led to a broad range of anomalies, where the overall impacts were not significantly different to the reference data. Methane flux anomalies showed a degree of variability in response to all types of extreme-events, as indicated by both positive and negatives anomalies in response to all event types. These conclusions remained consistent for non-normalized data (Figure S2 in Supporting Information S1). These results indicate that compound and discrete extreme-events influenced both the scale and direction of  $\text{CH}_4$  flux anomalies relative to the impacts of all-hot, all-cold, all-wet, all-dry extreme-events.

### 3.2.1. Seasonal Impacts Varied Across Extreme-Event Types

Seasonal differences in wetland impacts were observed in response to several types of extreme-events, namely dry-only, hot + dry, hot-only, and hot + wet extreme-events (Figure 5). Enhanced daily flux anomalies were found during summer (JJA) hot + dry extreme-events ( $1.36 \pm 1.47$ ) and hot-only extreme-events ( $0.45 \pm 1.06$ ) and, significantly different to the seasonal reference data. Conversely, summer cold-only extreme-events ( $-0.31 \pm 0.52$ ) caused significant negative flux anomalies relative to the reference data. Enhanced anomalies were also observed during summer hot + wet extreme-events ( $0.8 \pm 1.08$ ) though not significantly different to the reference data. Spring (MAM) hot + dry extreme-events ( $1.36 \pm 1.47$ ), dry-only extreme-events ( $0.45 \pm 1.49$ ), and hot-only extreme-events ( $0.16 \pm 0.58$ ) caused significant positive flux anomalies. The impacts of dry-only extreme-events showed large variability between seasons: notable positive anomalies during spring, varied anomalies during summer ( $-0.01 \pm 0.77$ ) and negative anomalies during autumn ( $-0.25 \pm 0.49$ ), with few or no measurements recorded during winter (DJF) extremes-events. Autumn (SON) extreme-events saw limited occurrence of significant flux anomalies relative to the reference data, where dry-only extreme-events and wet-only extreme-



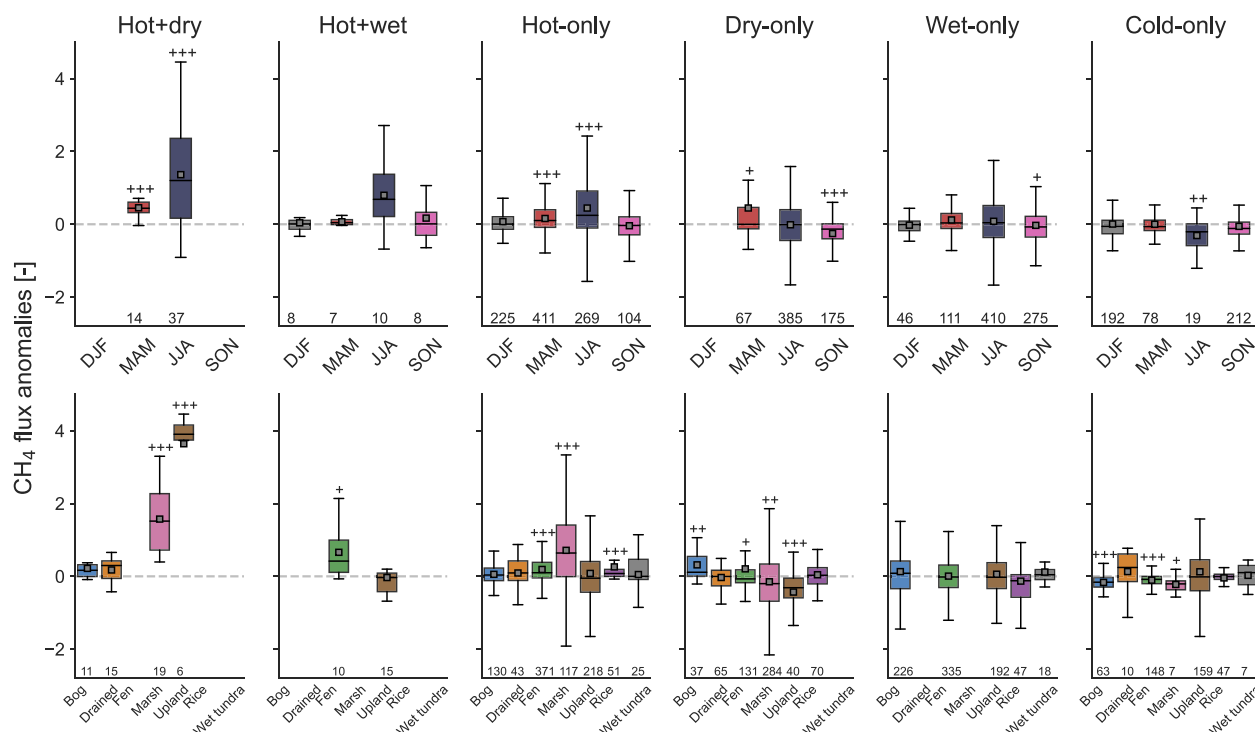


**Figure 5.** Extreme-event impacts varied across seasons (upper panels) and wetland classification (lower panels). Box plots show upper and lower quartile (boxes), median (black line), mean (gray square), smallest and largest values without outliers (whiskers). Statistical significance relative to the reference data (separated by season and wetland classification, respectively) is indicated by: +++ ( $p < 0.001$ ), ++ ( $p < 0.01$ ), + ( $p < 0.05$ ), calculated using Welch's  $t$ -test. The number of data points included in the analyses are written along the  $x$  axes. Distributions with less than five members are omitted.

events ( $-0.03 \pm 0.64$ ) are exceptions. Winter extreme-events did not cause significant impacts relative to the reference data. Seasonal differences were observed in response to several types of extreme-events, where summer and spring extreme-events led to particularly large effects relative to reference data (Figure 5).

### 3.2.2. Extreme-Event Impacts Varied According to Wetland Type

Extreme-event impacts varied depending on wetland type, where marsh sites tended to show a sensitivity to most types of extreme-events. Hot + dry extreme-events led to enhanced emissions in all types of wetlands, where, the effects were large and statistically significant in marsh ( $1.57 \pm 0.85$ ) and particularly, upland ( $3.64 \pm 1.01$ ) sites. Hot-only extreme-events generally led to varied effects, where enhanced and significant emissions were observed in marsh ( $0.71 \pm 1.08$ ), fen ( $0.19 \pm 0.48$ ), and rice ( $0.26 \pm 0.55$ ) sites. Whilst, bog ( $0.06 \pm 0.4$ ), drained ( $0.09 \pm 0.73$ ), wet tundra ( $0.05 \pm 0.73$ ) and upland ( $0.08 \pm 1.18$ ) sites showed a degree of variability in response to hot-only extreme-events. The impacts of hot + wet extreme-events led to diverging effects where emissions were notably enhanced in fens ( $0.66 \pm 0.73$ ) but variable in upland sites ( $-0.03 \pm 0.77$ ). Dry-only extreme-events led to a range of responses with small enhanced emissions in bog ( $0.32 \pm 0.54$ ) sites, negative anomalies in upland ( $-0.43 \pm 0.67$ ) sites, and small but variable anomalies in marsh ( $-0.15 \pm 0.85$ ), fen ( $0.21 \pm 1.12$ ), drained ( $-0.03 \pm 0.35$ ), and rice ( $0.04 \pm 0.42$ ) sites. This is partly due to differences in event durations observed across wetland types (Section 3.3). The impacts of cold-only extreme-events varied according to wetland type: mild but statistically significant negative anomalies in marshes ( $-0.22 \pm 0.25$ ), bogs ( $-0.17 \pm 0.22$ ), and fens ( $-0.11 \pm 0.2$ ), with minimal effects observed in drained ( $0.13 \pm 0.59$ ), upland ( $0.13 \pm 0.91$ ), wet tundra ( $0.03 \pm 0.36$ ), and rice ( $-0.04 \pm 0.29$ ) sites. Wet-only extreme-events did not lead to any statistically significant impacts. These results show that the effects of extreme-events differed depending on wetland type, where marsh sites tended to be sensitive to most types of extreme-events.

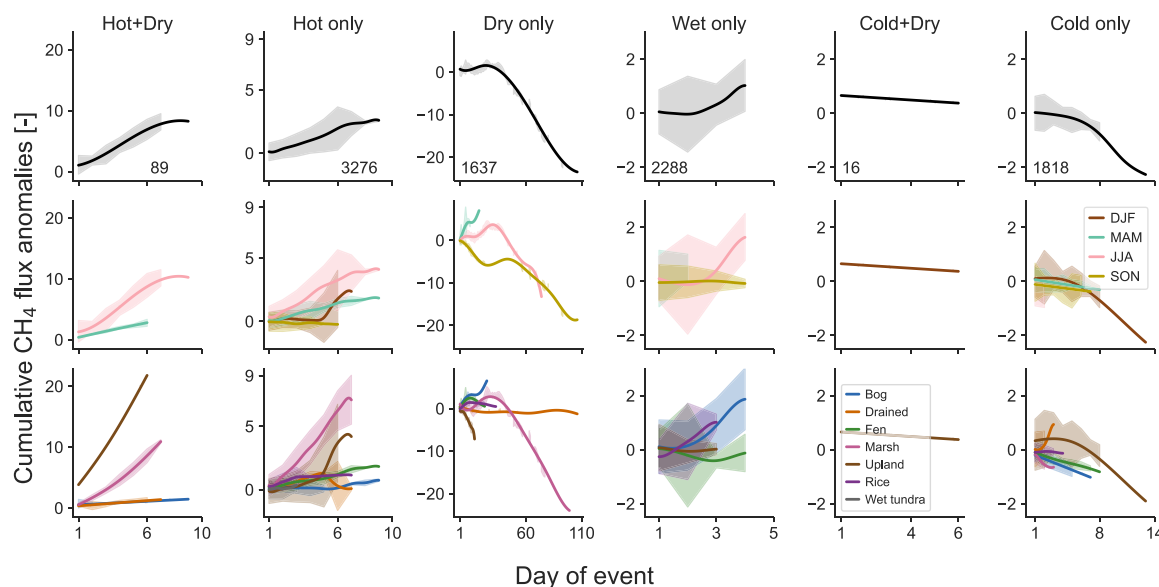


**Figure 6.** Extreme-event impacts varied over the event duration. Upper panels show the overall impacts, middle panels show the seasonal effects, and lower panels show the differences between wetland classification. Shading indicates  $\pm 1$  standard deviation. Generalized additive models were fitted to the data to display the overall trends. Extreme-event types with only single day extreme-events were omitted (cold + wet and hot + wet). Note the differing x and y axes.

### 3.3. Changing Impacts Over Event Duration

Cumulative impacts reveal the total emission anomaly caused by each type of extreme-event but also whether daily impacts remained consistent throughout the event duration. Extreme-events tended to lead to consistent effects on daily  $\text{CH}_4$  flux anomalies throughout the duration of the event, with the exception of dry-only events (Figure 6). The impacts of dry-only extreme-events on  $\text{CH}_4$  fluxes were marked by an initial phase of enhanced  $\text{CH}_4$  fluxes and a second phase of reduced fluxes, resulting in a large cumulative negative flux anomaly ( $-23.52$  on day 106, cumulative flux anomaly). It is worth noting that fluxes recorded during dry-only events that persisted beyond 100 days stem from 4 sites in the same region (US-Bi1, US-Bi2, US-Sne, US-Tw4). Hot + dry extreme-events ( $8.24$  on day 9) and hot-only extreme-events ( $2.6$  on day 9) caused consistent enhanced  $\text{CH}_4$  flux anomalies. Cold-only extreme-events ( $-2.2$  on day 14) resulted in consistent negative flux anomalies for the duration of the event. Cold + dry extreme-events led to positive daily flux anomalies ( $0.52 \pm 0.18$ , mean daily flux anomaly  $\pm$  standard deviation), that gently decreased in magnitude with the length of event, resulting in a very small cumulative flux anomaly ( $0.32$  on day 6). Wet-only extreme-events led to a small positive cumulative flux anomaly ( $1.03$  on day 4). These results indicated that extreme-events tended to cause consistent accumulating impacts throughout the event duration, with the exception of dry-only extreme-events where impacts occurred in two phases.

#### 3.3.1. Seasonality Influenced Cumulative Flux Anomalies

Seasonality influenced the magnitude of cumulative flux anomalies during all extreme-event types with available data (Figure 6). Particularly dry-only extreme-events which caused diverging impacts depending on season. Spring dry-only extreme-events caused consistently enhanced daily flux anomalies ( $6.95$  on day 18, cumulative flux anomaly). Whereas, summer dry-only extreme-events impacts occurred in two phases, shifting from enhanced to reduced fluxes on day 26, resulting in a large cumulative negative flux anomaly ( $-13.05$  on day 67). Autumn dry-only extreme-events caused consistently reduced fluxes, leading to a very large cumulative flux anomaly ( $-18.90$  on day 87). Summer hot-only extreme-events ( $4.11$  on day 9) and hot + dry ( $10.25$  on day 9) extreme-events caused large cumulative flux anomalies, with milder effects during spring, autumn, and winter. Hot-only extreme-events caused consistent positive flux anomalies during summer events ( $4.11$ ), winter events ( $2.37$ ), and spring events ( $1.84$ ). However, autumn hot-only extreme-events events led to small negative cumulative flux anomalies ( $-0.23$ ). Cold-only extreme-events caused negative daily flux anomalies across all seasons, with the largest cumulative anomalies occurring during winter ( $-2.08$ ). Spring, summer, and autumn

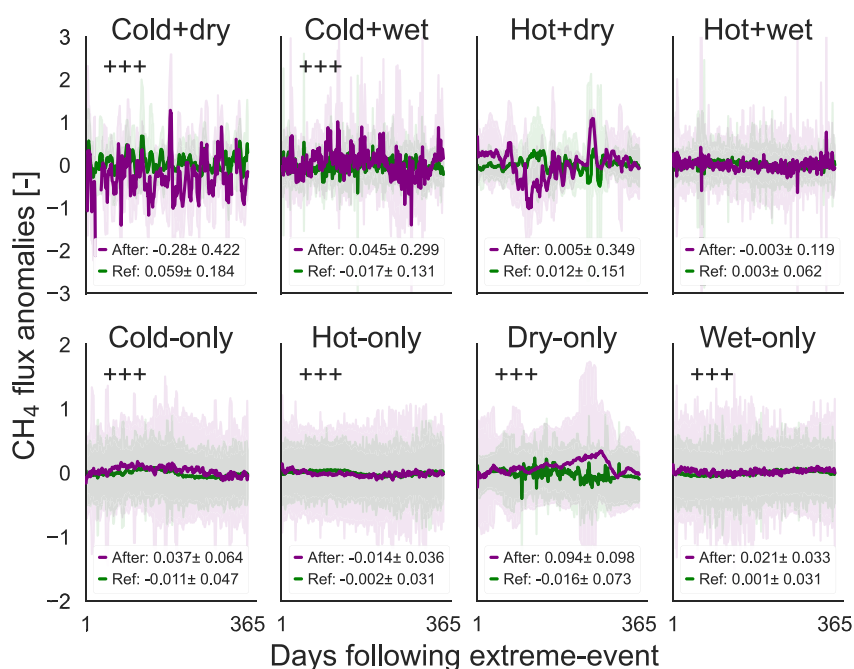


**Figure 7.** Lagged impacts following extreme-events lead to enhanced flux variability. Flux anomalies are plotted for the 12 months after the extreme-event (averaged across all sites and extreme-events). Day 1 is the first day following the end of the extreme-event. Statistical significance relative to the reference period is indicated by: +++ ( $p < 0.001$ ), ++ ( $p < 0.01$ ), + ( $p < 0.05$ ), calculated using a Mann–Whitney U test. The mean  $\pm$  STD of the mean daily  $\text{CH}_4$  flux anomalies of the year following extreme-events and the reference data are provided in the legend, and shading indicates  $\pm 1$  STD. The number of  $\text{CH}_4$  measurements used to make this figure is plotted in Figure S4 in Supporting Information S1.

cold-only extreme-events led to small negative cumulative flux anomalies ( $-0.37$ ,  $-0.49$ ,  $-0.45$ , respectively). Both summer and spring hot + dry extreme-events resulted in consistent enhanced flux anomalies. Wet-only extreme-events caused consistent enhanced anomalies during summer (1.65) and spring (0.50). These results showed that seasonality influenced the cumulative and changing impacts over the extreme-event duration, but caused polarizing effects during dry-only extreme-events.

### 3.3.2. Cumulative Impacts Varied According to Wetland Type

Cumulative extreme-event impacts varied according to wetland type. In response to hot + dry extreme-events, accumulated  $\text{CH}_4$  anomalies were substantial in upland (21.85) and marsh (10.94) sites but minimal in bog (1.47) and drained (1.29) sites. Over the course of dry-only extreme-events, large negative anomalies accumulated in marsh sites ( $-23.62$ ), moderate negative anomalies accumulated in upland sites ( $-7.29$ ), enhanced anomalies in bog sites (6.11), and small anomalies in fens (2.55), rice (1.53), and drained ( $-1.62$ ) sites. While both drained and marsh sites recorded  $\text{CH}_4$  measurements during long duration ( $>80$  days) dry-only extreme-events, large anomalies were only observed in marsh sites. Over the duration of hot-only extreme-events, enhanced emissions accumulated at marsh (7.1) and upland (4.19) sites, while small but consistent emissions were observed at fen (1.83), rice (1.15), drained (1.23) and bog (0.74) sites. The emissions that accumulated over even the most persistent (4 days) wet-only extreme-events were low across all types of wetlands, with the largest anomalies observed in bog sites (1.88). During cold-only extreme-events, small or no anomalies were observed in most types of wetlands, where the largest effects, as well as longest event durations, were observed in upland sites ( $-1.73$ ).

### 3.4. Lagged Response: Enhanced Flux Variability Following Extreme-Events

For at least the year following extreme-events,  $\text{CH}_4$  fluxes were observed to be highly variable and significantly different ( $p < 0.001$ ) to the reference data for several extreme-event types (Figure 7), with the largest effects observed following cold + dry extreme-events. Of the discrete extreme-event types, dry-only extreme-events exerted the largest anomalies in the year following events, in comparison to the reference data. Methane flux

anomalies following cold + wet extreme-events ( $0.05 \pm 0.3$ , mean daily flux anomaly  $\pm$  standard deviation), cold-only extreme-events ( $0.04 \pm 0.06$ ), and dry-only extreme-events ( $0.09 \pm 0.1$ ) were higher than the reference data, whereas  $\text{CH}_4$  fluxes following cold + dry extreme-events ( $-0.28 \pm 0.42$ ) and hot-only extreme-events ( $-0.04 \pm 0.04$ ) were reduced relative to the reference data. Methane fluxes following wet-only extreme-events ( $0.02 \pm 0.03$ ), were significantly different to the reference data ( $0.001 \pm 0.03$ ). Fluxes exhibited increased variability in the year following hot + dry extreme-events and hot + wet extreme-events, although average annual  $\text{CH}_4$  flux anomalies were comparable to the reference data. These results are indicative of the lasting effects extreme-events can have on wetland ecosystems.

## 4. Discussion

### 4.1. Assessment of Compound and Discrete Extreme-Events

We found that differentiating extreme-events into compound and discrete events to be a critical step to understanding the extreme-event impacts on wetland ecosystems because compound extreme-events can have impacts on  $\text{CH}_4$  fluxes that are opposite in sign to discrete extreme-events. Hot + dry extreme-events led to large enhanced  $\text{CH}_4$  fluxes which were significantly different to both dry-only and hot-only extreme-events, indicating that interacting processes caused by concurrent extreme-events work to enhance net  $\text{CH}_4$  emissions. This was also true for the compounding and interacting processes during cold + wet extreme-events relative to all-cold and all-wet extreme-events.

Our results indicate that compound and discrete extreme hot events (hot-only, hot + wet) and extreme dry events (hot + dry, dry-only) lead to large impacts on wetland  $\text{CH}_4$  emissions, where extreme wet events (wet-only), and extreme cold events (cold-only) generally have mild effects. Many previous studies have found temperature to be the main driver of daily  $\text{CH}_4$  fluxes at wetland sites (Desai et al., 2015; Sturtevant et al., 2016). Daily soil and air temperature were identified as the dominant predictors of  $\text{CH}_4$  emissions at FLUXNET- $\text{CH}_4$  sites (Knox et al., 2021; Sturtevant et al., 2016). Methane fluxes are reduced during cold + wet extreme-events which indicates that the sensitivity of methanogenic archaea to cool temperatures is greater than the impacts of increased oxic conditions (Bardgett et al., 2008; Conrad, 1996). It is unexpected that cold + dry extreme-events did not lead to anomalous  $\text{CH}_4$  fluxes, given that cold temperatures suppress fermentation and dry conditions promote  $\text{CH}_4$  oxidation by increasing oxygen availability and methanotrophic activity (Dean et al., 2018). However, limited flux measurements were recorded during cold + dry extreme-events, and of those available, all were recorded during winter where  $\text{CH}_4$  emissions are typically very low.

We assessed the impact of heavy rainfall extreme-events but did not find a consistent relationship with anomalous  $\text{CH}_4$  fluxes, where autumn wet-only extreme-events were an exception. Whilst the anaerobic conditions resulting from saturated soils stimulate methanogenic activity and promote heightened  $\text{CH}_4$  production (Dean et al., 2018), previous multi-site syntheses have not found a direct relationship between daily precipitation and wetland  $\text{CH}_4$  emissions (Knox et al., 2021). However, heavy precipitation days have been found to be a key driver of wetland  $\text{CH}_4$  emissions in land surface models (Xu et al., 2024). Until now, no multi-site synthesis has confirmed whether heavy precipitation events affect observed wetland  $\text{CH}_4$  emissions. This assessment shows that overall, even the most extreme precipitation events do not impact wetland  $\text{CH}_4$  emissions. Therefore, this insight can help improve the representation of wetland  $\text{CH}_4$  emission processes in land surface models (Forbrich et al., 2024).

There are two possible explanations for the lack of a relationship between heavy precipitation events and  $\text{CH}_4$  anomalies. Firstly, heavy precipitation events may not lead to an increase in local anaerobic conditions. Precipitation may not have a direct impact on site water levels which are also dependent on evapotranspiration, and local site topography, amongst other factors. Secondly, enhanced methanogenesis may have occurred, and contributed to the belowground  $\text{CH}_4$  pool, without impacting surface emissions, due to the time required to replenish soil  $\text{CH}_4$  concentrations (Reiche et al., 2009). Previous studies have found that  $\text{CH}_4$  emissions lag behind water table depth (WTD) by a period of 17 days (Knox et al., 2021) or 10–11 days (Goodrich et al., 2015; Moore & Roulet, 1993).

Previous multi-site syntheses of similar site data sets have primarily investigated the impacts of isolated drivers on wetland  $\text{CH}_4$  emissions (Chang et al., 2021; Feron et al., 2024; Knox et al., 2021; Li et al., 2023). Our study indicates that co-occurring anomalous drivers can lead to unprecedented wetland  $\text{CH}_4$  emissions. For example, hot + dry extreme-events led to enhanced emissions, where the impacts were greater and significantly different to

the impacts related to hot-only and dry-only extreme-events. Similarly cold + wet extreme-events led to reduced emissions, with effects that were larger and significantly different to those of cold-only and wet-only extreme-events. These findings suggest that future multi-site syntheses can gain further insights by including assessments of interacting drivers.

#### 4.2. Consistent Impacts Throughout Most Extreme-Events

Overall, most types of extreme-events caused consistent impacts on cumulative CH<sub>4</sub> flux anomalies throughout the duration of the event, where dry-only extreme-events were an exception. Dry-only extreme-events led to contrasting effects on CH<sub>4</sub> fluxes (Section 3.3). It is commonly understood that periods of extreme dryness lead to reduced CH<sub>4</sub> fluxes due to larger aerobic soil space, enhanced methanotrophic and reduced methanogenic activity (Borken et al., 2006; Knorr & Blodau, 2009). However, this assessment revealed that the impacts of dry-only extreme-events occur in two phases, where, the first days of the event are marked by increased CH<sub>4</sub> fluxes and the last days are marked by reduced CH<sub>4</sub> fluxes. Experimental drought studies have observed initial pulses of high CH<sub>4</sub> release, followed by no or low CH<sub>4</sub> emissions (Dowrick et al., 2006; Estop-Aragonés et al., 2016). Previously produced CH<sub>4</sub> hitherto trapped in the saturated soil structure can diffuse upwards through the newly aerated soil column or be released as ebullition due to a decrease in pressure. The newly oxic soil layers become unsuitable for further CH<sub>4</sub> production, allowing for continued CH<sub>4</sub> oxidation (Dowrick et al., 2006); a process likely responsible for the reduced CH<sub>4</sub> fluxes in the later stage of dry-only events.

#### 4.3. Seasonal Differences

The impacts of dry-only, hot-only, and hot + dry extreme-events on daily CH<sub>4</sub> flux anomalies varied depending on season (Sections 3.2.1 and 3.3.1). Methane emissions are closely coupled to seasonal plant productivity at sites with plants containing aerenchyma tissue (van den Berg et al., 2020; Vroom et al., 2022), but decoupled at other sites due to slower diffusive transport or storage effects (Pirk et al., 2015; Treat et al., 2018). Seasonal effects were particularly strong for dry-only extreme-events, which caused increased emissions in spring, varied effects in summer, and decreased emissions in autumn. Several summer extreme-event occurrences caused significant differences relative to the summer reference flux anomalies, indicating that CH<sub>4</sub> emissions are more sensitive to temperature changes in warmer months (Li et al., 2023).

The cumulative effects of extreme-events varied depending on season, particularly during dry-only extreme-events. Enhanced flux anomalies were observed during spring dry-only events, variable during summer events, and reduced during autumn events. Rhizodeposition which produces the primary substrate for methanogenesis, is closely coupled with photosynthetic activity, and therefore strongest in spring and summer (Jones et al., 2004). Reduced rhizodeposition in autumn may limit the capacity for below-ground CH<sub>4</sub> production, negating enhanced CH<sub>4</sub> flux anomalies observed during the initial phase of spring and summer dry-only events. Future analyses may investigate the role of preceding site conditions (e.g., water table levels), related to seasonal evapotranspiration cycles, on wetland CH<sub>4</sub> fluxes during extreme dry periods (Reiche et al., 2009).

#### 4.4. The Role of Wetland Type

Wetland types varied widely in their sensitivity to extreme-events, where marsh and upland sites were generally most sensitive to extreme-events and drained sites were least sensitive to extreme-events. Wetland classification is based on environmental factors such as soil composition (peat or permafrost), nutrient status (nutrient-poor or nutrient-rich), water source (precipitation-fed, groundwater-fed, or a combination), elevation (upland or not), snow presence, and vegetation type (Treat et al., 2018). These environmental properties are catalysts within a number of relevant biogeochemical processes related to temperature, precipitation and water level, and substrate availability that play a role in both CH<sub>4</sub> production and oxidation (Olefeldt et al., 2012). These results show that both drained wetlands and marshes experience long periods of drought (i.e., > 80 days). However, the impact on marshes is substantially greater than the impacts on drained wetlands. As expected, drained wetlands were not found to be sensitive to extreme-events, likely due to their low water tables and consequently, low CH<sub>4</sub> production potential (Turetsky et al., 2014). Marshes, however, generally have nutrient rich soils and may contain aerenchyma vegetation, which efficiently transport CH<sub>4</sub> between the soil and the atmosphere, meaning changes to belowground CH<sub>4</sub> concentrations are quickly evident in the surface flux. Upland sites were found to be sensitive to extreme-events, despite being typically associated with low annual CH<sub>4</sub> budgets (Olefeldt et al., 2013; Voigt



et al., 2017). Their heightened sensitivity may be attributed to their localized extent at high elevations, where upland systems are often adapted to specific and unique conditions, making them more susceptible to changes in temperature and water levels (Knox et al., 2019). Both fens and bogs showed some sensitivity to extreme-events, despite fens generally exhibiting large annual CH<sub>4</sub> budgets relative to bogs (Knox et al., 2019; Treat et al., 2018). Fens and bogs typically have substantial water-holding and thermal capacities because of their deep soils, due to the presence of Sphagnum vegetation and peat accumulation, potentially making them less sensitive to short lived changes in temperature, heavy precipitation, and drought. However, disruption to their nutrient levels or vegetation communities can lead to substantial long-term, lagged effects. Permafrost and carbon-rich tundra soils may exhibit different CH<sub>4</sub> flux dynamics compared to other wetland systems because the presence of permafrost can reduce the active soil layer, and thereby the maximum volume of the soil gas reservoir, facilitating the rapid release of elevated soil CH<sub>4</sub> concentrations (Bao et al., 2023; Pirk et al., 2015). Future studies may investigate the ecological factors that make marshes and upland sites more sensitive to extreme-events, and determine whether this finding is consistent for extreme-events defined across other spatial and temporal scales.

#### 4.5. Significant Lagged Effects at Least One Year After Extreme-Events

For at least 1 year following several types of extreme-events, CH<sub>4</sub> fluxes were significantly different to the reference data (Section 3.4), where cold + dry extreme-events showed the largest lagged effects. Lagged effects can include diminished ecosystem resistance to environmental stress, changes in rhizodeposition, effects on soil properties, and shifts in plant and microbial populations (Frank et al., 2015). Vascular plants with large aerenchyma tissue are fast growing, competitive vegetation, capable of out-competing slow growing species such as Sphagnum mosses (Harpenslager et al., 2015) whilst efficiently transporting belowground CH<sub>4</sub> into the atmosphere (van den Berg et al., 2020). Future research may investigate if and how climate change and extreme-events may lead to shifts in wetland vegetation composition. Of the discrete extreme-event types, dry-only extreme-events caused the largest lagged impacts. A delay of methanogenic CH<sub>4</sub> production often occurs following drought resulting in persistent reduced CH<sub>4</sub> emissions (Dowrick et al., 2006; Estop-Aragonés et al., 2013). This may be due to a change in electron acceptor availability (Freeman et al., 2004; Knorr & Blodau, 2009) which enable competing microbial populations to out-compete methanogens for available carbon substrates, reducing methanogenic activity in (re)saturated soils, and consequently reducing CH<sub>4</sub> emissions (Angel et al., 2012; Yuan et al., 2019). Competition for substrates is a key factor influencing the rate of CH<sub>4</sub> production in wetland systems. Long-term lag effects following extreme climate events have been documented (Bastos, Ciais, et al., 2020; Desai, 2014; Zhao et al., 2016) and carbon-rich systems, such as wetlands, are at particular risk due to the long recovery time required to regain lost carbon stocks (Frank et al., 2015).

Extreme-events, as defined in this study, may occur in anomalously warm years or seasons, affecting CH<sub>4</sub> fluxes beyond the length of an extreme-event. The method used in this study to assess lagged impacts does not account for possible confounding large-scale drivers, however, this analysis provides preliminary insights into the impacts of lagged effects following extreme-events.

#### 4.6. Longterm Trends of Extreme-Event Impacts

Extreme event impacts on wetlands are changing due to changes in the intensity and frequency of extreme-events (Dunn et al., 2020; Seneviratne et al., 2012), changing site characteristics (Bao et al., 2023; Parmentier et al., 2018), and anthropogenic interventions (Kosten et al., 2018). Beyond this, extreme-event impacts are also changing due to non-linear interactions between drivers and processes (Knox et al., 2021; Sturtevant et al., 2016). Human-caused climate change is now altering the behavior of large scale drivers of interannual variability (such as the North Atlantic Oscillation, El Nino Southern Oscillation and others), affecting the occurrence and intensity of extreme temperature and precipitation (or drought) events (Abram et al., 2021; Renom et al., 2011). The longterm trends of extreme-event occurrences at wetland sites included in this study indicate increasing instances of enhanced CH<sub>4</sub> fluxes in response to hot-only extreme-events and hot + wet extreme-events whilst negative trends indicate fewer instances of reduced CH<sub>4</sub> fluxes during cold-only extreme-events (Section 3.1). These trends indicate that wetlands may increasingly contribute to the rise in atmospheric CH<sub>4</sub> concentrations, providing a positive feedback to climate warming (Feron et al., 2024; Nisbet et al., 2023).

Seasonal differences in the long-term trends of extreme-event occurrence (Figure S5 in Supporting Information S1) are consistent with increasing surface temperatures, where observations show that minimum (winter)

temperatures are increasing faster than maximum (summer) temperatures (Dunn et al., 2020). Significant positive trends indicate greater occurrences of enhanced CH<sub>4</sub> fluxes during both summer hot-only and hot + dry extreme-events. European summer heatwaves are expected to occur more often in response to climate change due to a poleward shift in the North Hemisphere atmospheric jet stream (Horton et al., 2015). Simultaneous hot and dry periods are projected to occur more frequently across Europe, the Mediterranean and other areas due to alteration of the North Atlantic Oscillation north-south dipole pattern (Hao et al., 2022) and was already observed to be a key mechanism driving the 2016/17 European drought (García-Herrera et al., 2019). Alongside this, negative trends indicate fewer occurrences of reduced fluxes during both summer cold-only extreme-events and spring dry-only extreme-events. Observed trends indicate an increasing frequency of winter hot + wet and hot-only extreme-events, and a decreasing frequency of winter cold-only extreme-events, however, winter extreme-events are unaccompanied by significant CH<sub>4</sub> flux anomalies. Hot extreme-events during winter can induce plant activity, leading to direct plant damage when temperatures return to below freezing, a phenomenon that has been called “false spring” (Frank et al., 2015). Observed spring extreme-event trends indicate increasing frequency of enhanced CH<sub>4</sub> fluxes during hot-only extreme-events and hot + dry extreme-events. Spring thaw in high latitude systems cause substantial CH<sub>4</sub> emissions which can account for one quarter of annual CH<sub>4</sub> emissions (Bao et al., 2021; Long et al., 2010), and therefore an increase to the frequency of spring hot extreme-events could impact annual CH<sub>4</sub> budgets. These trends indicate that summer and spring are witnessing the greatest changes to extreme-event driven wetland CH<sub>4</sub> emissions with greater occurrences of enhanced fluxes during spring and summer hot-only and hot + dry extreme-events (Feron et al., 2024). Conversely summer is experiencing fewer occurrences of reduced fluxes during cold-only extreme-events whilst spring is witnessing fewer occurrences of reduced fluxes during dry-only extreme-events. These trends indicate that wetlands are experiencing a rise in the frequency of extreme-events that amplify CH<sub>4</sub> emissions whilst simultaneously witnessing a decline in the types of extreme-events that reduce emissions. This highlights the growing potential for wetlands to increasingly contribute to atmospheric CH<sub>4</sub> concentrations, acting as a positive feedback mechanism that accelerates climate warming (Feron et al., 2024; Zhang et al., 2023).

#### 4.7. Further Investigations

The results of this research highlight the importance of using both compound and discrete extreme-event definitions when investigating ecosystem extreme-event impacts. Exploration of alternative variables which are inherently compound in nature, such as water level or vapor pressure deficit, may be useful signifiers of extreme-events critical to wetlands. Our assessment of extreme precipitation impacts on wetland CH<sub>4</sub> emissions is limited in scope because the impacts of changing precipitation on wetland water levels and CH<sub>4</sub> emissions are dependent on a number of other factors such as evapotranspiration and topography. Whilst data sets of global surface water extent (Jensen & McDonald, 2019) and soil moisture (Lal et al., 2023) already exist and there are ongoing advancements of WTD estimates (Burdun et al., 2023), there are currently no data sets of global daily water levels. Such a data set is urgently needed. However, to validate long term water level estimates there is also a need for in situ site water level data. Only half of the sites included in this study provide in situ water level measurements. Therefore, the availability of both longterm global data sets and in situ site data limit the capacity to perform multi-site assessments of extreme water level impacts.

This study has taken the approach of first identifying anomalous drivers and secondly assessing related ecosystem impacts. This approach takes advantage of readily available meteorological and EC flux data. However, an alternative method is to first define ecosystem extreme-events by identifying extreme flux anomalies for example, and subsequently undertake further analysis to attribute the drivers or processes responsible (Zscheischler et al., 2013, 2014).

The difficulties faced by EC towers when measuring CH<sub>4</sub> fluxes during rainfall extreme-events (Burns et al., 2015) limits the temporal coverage of site data, potentially obscuring the full impact of wet extreme-events. Flux towers are unable to operate during moments of rainfall and therefore, these moments are omitted from the site measurement record. Our own aggregation of data, required 70% of half-hourly data or data associated with the highest QC flag. However, no large anomalies were observed in response to heavy precipitation extreme-events and it is therefore unlikely to have caused a bias in the data. Notably, we did not account for dissolved CH<sub>4</sub> lost by runoff, which may be an important transport pathway (Dinsmore et al., 2010).

Additionally, regional gaps in site locations contributed to spatial discrepancies in the analysis and temporal gaps in site measurements led to a low availability of winter flux measurements, particularly for high latitude sites. There was a lack of both tropical sites and southern hemisphere sites in this study, highlighting the urgent need for more observational sites in these regions (Schwalm et al., 2010).

## 5. Conclusions

Changing wetland CH<sub>4</sub> emissions are responsible for recent increases in global CH<sub>4</sub> emissions. Whilst extreme climate events are changing in both frequency and intensity, little is known about their impacts on wet ecosystems. This study finds that the effects of compound extreme-events (e.g., hot + dry extreme-events) on daily CH<sub>4</sub> fluxes are greater in magnitude than discrete extreme events (e.g., hot-only). In general, heavy precipitation events did not lead to CH<sub>4</sub> flux anomalies, however, per event dry-only extreme-events led to substantial cumulative negative anomalies due to their extended duration. These two points together provide critical insights into the impacts of the changing precipitation cycle on wetland CH<sub>4</sub> emissions and how we can expect future extreme-events to impact wetland CH<sub>4</sub> emissions. Longterm lagged responses can persist for at least the year following extreme-events. Looking ahead, these findings have implications for understanding how extreme-events may evolve in the context of climate change. As winters continue to warm faster than summers, we can expect fewer occurrences of reduced CH<sub>4</sub> fluxes during cold-only extreme-events, and increasing occurrences of enhanced CH<sub>4</sub> fluxes in response to hot-only extreme-events, and hot + wet extreme-events. This assessment provides land surface modelers the opportunity to test simulated wetland responses to extreme compound and discrete events. These results highlight the importance of the assessment of compound and discrete extreme-events when investigating ecosystem impacts.

## Conflict of Interest

The authors declare no conflicts of interest relevant to this study.

## Data Availability Statement

This work used data publicly available through FLUXNET-CH<sub>4</sub> (Delwiche et al., 2021; Knox et al., 2019), Ameriflux (Novick et al., 2018), GPCC (Schamm et al., 2014; Ziese et al., 2018), and ERA5-Land (Muñoz-Sabater et al., 2021). All related data are publicly available for download through the respective websites.

## Acknowledgments

TJRL was supported by Horizon Europe AVENGERS (101081322). We thank Alex Buzacott for insightful discussions on the functionality of EC towers and Sander Veraverbeke for valuable discussions in the early development stage of this project. We thank the following sites for making their site data records publicly available: BR-Npw, CA-DBB, CA-SCB, CA-SCC, CH-Cha, DE-Hte, DE-Zrk, FI-Lom, FI-Si2, FI-Sii, JP-BBY, KR-CRK, NZ-Kop, RU-Cok, RU-Fy2, SE-Deg, US-A03, US-A10, US-Atq, US-BZB, US-BZF, US-Bi1, US-Bi2, US-DPW, US-EML, US-Ho1, US-ICs, US-Ivo, US-Los, US-MBP, US-Myb, US-NC4, US-NGB, US-NGC, US-ORv, US-PFa, US-Snd, US-Sne, US-Srr, US-SJ, US-Tw1, US-Tw3, US-Tw4, US-Twt, US-Uaf.

## References

- Abram, N. J., Henley, B. J., Gupta, A. S., Lippmann, T. J., Clarke, H., Dowdy, A. J., et al. (2021). Connections of climate change and variability to large and extreme forest fires in southeast Australia. *Communications Earth and Environment*, 2(1), 8. <https://doi.org/10.1038/s43247-020-00065-8>
- Angel, R., Kammann, C., Claus, P., & Conrad, R. (2012). Effect of long-term free-air CO<sub>2</sub> enrichment on the diversity and activity of soil methanogens in a periodically waterlogged grassland. *Soil Biology and Biochemistry*, 51, 96–103. <https://doi.org/10.1016/j.soilbio.2012.04.010>
- Aschrott, P. L. (2021). Theil (Vol. 1). <https://doi.org/10.1515/9783112603840-001>
- Bao, T., Jia, G., & Xu, X. (2023). Weakening greenhouse gas sink of pristine wetlands under warming. *Nature Climate Change*, 13(5), 462–469. <https://doi.org/10.1038/s41558-023-01637-0>
- Bao, T., Xu, X., Jia, G., Billesbach, D. P., & Sullivan, R. C. (2021). Much stronger tundra methane emissions during autumn freeze than spring thaw. *Global Change Biology*, 27(2), 376–387. <https://doi.org/10.1111/gcb.15421>
- Bardgett, R. D., Freeman, C., & Ostle, N. J. (2008). Microbial contributions to climate change through carbon cycle feedbacks. *ISME Journal*, 2(8), 805–814. <https://doi.org/10.1038/ismej.2008.58>
- Bastos, A., Ciais, P., Friedlingstein, P., Sitch, S., Pongratz, J., Fan, L., et al. (2020a). Direct and seasonal legacy effects of the 2018 heat wave and drought on European ecosystem productivity. *Science Advances*, 6(24), 1–14. <https://doi.org/10.1126/sciadv.aba2724>
- Bastos, A., O'Sullivan, M., Ciais, P., Makowski, D., Sitch, S., Friedlingstein, P., et al. (2020b). Sources of uncertainty in regional and global terrestrial CO<sub>2</sub> exchange estimates. *Global Biogeochemical Cycles*, 34(2), 1–21. <https://doi.org/10.1029/2019GB006393>
- Borken, W., Davidson, E. A., Savage, K., Sundquist, E. T., & Steudler, P. (2006). Effect of summer throughfall exclusion, summer drought, and winter snow cover on methane fluxes in a temperate forest soil. *Soil Biology and Biochemistry*, 38(6), 1388–1395. <https://doi.org/10.1016/j.soilbio.2005.10.011>
- Bragazza, L. (2008). A climatic threshold triggers the die-off of peat mosses during an extreme heat wave. *Global Change Biology*, 14(11), 2688–2695. <https://doi.org/10.1111/j.1365-2486.2008.01699.x>
- Burdun, I., Bechtold, M., Aurela, M., De Lannoy, G., Desai, A. R., Humphreys, E., et al. (2023). Hidden becomes clear: Optical remote sensing of vegetation reveals water table dynamics in northern peatlands. *Remote Sensing of Environment*, 296(July), 113736. <https://doi.org/10.1016/j.rse.2023.113736>
- Burns, S. P., Blanken, P. D., Turnipseed, A. A., Hu, J., & Monson, R. K. (2015). The influence of warm-season precipitation on the diel cycle of the surface energy balance and carbon dioxide at a Colorado subalpine forest site. *Biogeosciences*, 12(23), 7349–7377. <https://doi.org/10.5194/bg-12-7349-2015>

- Chang, K. Y., Riley, W. J., Knox, S. H., Jackson, R. B., McNicol, G., Poulter, B., et al. (2021). Substantial hysteresis in emergent temperature sensitivity of global wetland CH<sub>4</sub> emissions. *Nature Communications*, 12(1), 2266. <https://doi.org/10.1038/s41467-021-22452-1>
- Christensen, T. R., Lund, M., Skov, K., Abermann, J., López-Blanco, E., Scheller, J., et al. (2021). Multiple ecosystem effects of extreme weather events in the arctic. *Ecosystems*, 24(1), 122–136. <https://doi.org/10.1007/s10021-020-00507-6>
- Conrad, R. (1996). Soil microorganisms as controllers of atmospheric trace gases (H<sub>2</sub>, CO, CH<sub>4</sub>, OCS, N<sub>2</sub>O, and NO). *Microbiological Reviews*, 60(4), 609–640. <https://doi.org/10.1128/mmbr.60.4.609-640.1996>
- Davidson, E. A., Nepstad, D. C., Ishida, F. Y., & Brando, P. M. (2008). Effects of an experimental drought and recovery on soil emissions of carbon dioxide, methane, nitrous oxide, and nitric oxide in a moist tropical forest. *Global Change Biology*, 14(11), 2582–2590. <https://doi.org/10.1111/j.1365-2486.2008.01694.x>
- Dean, J. F., Middelburg, J. J., Röckmann, T., Aerts, R., Blauw, L. G., Egger, M., et al. (2018). Methane feedbacks to the global climate system in a warmer world. *Reviews of Geophysics*, 56(1), 207–250. <https://doi.org/10.1002/2017RG000559>
- Delwiche, K. B., Knox, S. H., Malhotra, A., Fluet-Chouinard, E., McNicol, G., Feron, S., et al. (2021). FLUXNET-CH<sub>4</sub>: A global, multi-ecosystem dataset and analysis of methane seasonality from freshwater wetlands. *Earth System Science Data*, 13(7), 3607–3689. <https://doi.org/10.5194/essd-13-3607-2021>
- Desai, A. R. (2014). Influence and predictive capacity of climate anomalies on daily to decadal extremes in canopy photosynthesis. *Photosynthesis Research*, 119(1–2), 31–47. <https://doi.org/10.1007/s11120-013-9925-z>
- Desai, A. R., Xu, K., Tian, H., Weishampel, P., Thom, J., Baumann, D., et al. (2015). Landscape-level terrestrial methane flux observed from a very tall tower. *Agricultural and Forest Meteorology*, 201, 61–75. <https://doi.org/10.1016/j.agrformet.2014.10.017>
- Dinsmore, K. J., Billett, M. F., Skiba, U. M., Rees, R. M., Drewer, J., & Helfter, C. (2010). Role of the aquatic pathway in the carbon and greenhouse gas budgets of a peatland catchment. *Global Change Biology*, 16(10), 2750–2762. <https://doi.org/10.1111/j.1365-2486.2009.02119.x>
- Dowrick, D. J., Freeman, C., Lock, M. A., & Reynolds, B. (2006). Sulphate reduction and the suppression of peatland methane emissions following summer drought. *Geoderma*, 132(3–4), 384–390. <https://doi.org/10.1016/j.geoderma.2005.06.003>
- Du, H., Alexander, L. V., Donat, M. G., Lippmann, T., Srivastava, A., Salinger, J., et al. (2019). Precipitation from persistent extremes is increasing in most regions and globally. *Geophysical Research Letters*, 46(11), 6041–6049. <https://doi.org/10.1029/2019GL081898>
- Dunn, R. J., Alexander, L. V., Donat, M. G., Zhang, X., Bador, M., Herold, N., et al. (2020). Development of an updated global land in situ-based data set of temperature and precipitation extremes: HadEX3. *Journal of Geophysical Research: Atmospheres*, 125(16), 1–28. <https://doi.org/10.1029/2019JD032263>
- Estop-Aragónés, C., Knorr, K. H., & Blodau, C. (2013). Belowground in situ redox dynamics and methanogenesis recovery in a degraded fen during dry-wet cycles and flooding. *Biogeosciences*, 10(1), 421–436. <https://doi.org/10.5194/bg-10-421-2013>
- Estop-Aragónés, C., Zajac, K., & Blodau, C. (2016). Effects of extreme experimental drought and rewetting on CO<sub>2</sub> and CH<sub>4</sub> exchange in mesocosms of 14 European peatlands with different nitrogen and sulfur deposition. *Global Change Biology*, 22(6), 2285–2300. <https://doi.org/10.1111/gcb.13228>
- Farlie, D. J. G., & Kendall, M. G. (1971). Rank correlation methods. In *Journal of the royal statistical society. Series A (general)*, (Vol. 134(4), p. 682). Charles Griffin. <https://doi.org/10.2307/2343668>
- Feron, S., Malhotra, A., Bansal, S., Fluet-Chouinard, E., McNicol, G., Knox, S. H., et al. (2024). Recent increases in annual, seasonal, and extreme methane fluxes driven by changes in climate and vegetation in boreal and temperate wetland ecosystems. *Global Change Biology*, 30(1), 1–18. <https://doi.org/10.1111/gcb.17131>
- Forbrich, I., Yazbeck, T., Sulman, B., Morin, T. H., Tang, A. C. I., & Bohrer, G. (2024). Three decades of wetland methane surface flux modeling by earth system models—advances, applications, and challenges. *Journal of Geophysical Research: Biogeosciences*, 129(3). <https://doi.org/10.1029/2023JG007915>
- Frank, D., Reichstein, M., Bahn, M., Thonicke, K., Frank, D., Mahecha, M. D., et al. (2015). Effects of climate extremes on the terrestrial carbon cycle: Concepts, processes and potential future impacts. *Global Change Biology*, 21(8), 2861–2880. <https://doi.org/10.1111/gcb.12916>
- Freeman, C., Fenner, N., Ostle, N. J., Kang, H., Dowrick, D. J., Reynolds, B., et al. (2004). Export of dissolved organic carbon from peatlands under elevated carbon dioxide levels. *Nature*, 430(6996), 195–198. <https://doi.org/10.1038/nature02707>
- García-Herrera, R., Garrido-Pérez, J. M., Barriopedro, D., Ordóñez, C., Vicente-Serrano, S. M., Nieto, R., et al. (2019). The European 2016/17 drought. *Journal of Climate*, 32(11), 3169–3187. <https://doi.org/10.1175/JCLI-D-18-0331.1>
- Goodrich, J. P., Campbell, D. I., Roulet, N. T., Clearwater, M. J., & Schipper, L. A. (2015). Overriding control of methane flux temporal variability by water table dynamics in a Southern Hemisphere, raised bog. *Journal of Geophysical Research: Biogeosciences*, 120(5), 819–831. <https://doi.org/10.1002/2014JG002844>
- Hao, Z., Hao, F., Xia, Y., Feng, S., Sun, C., Zhang, X., et al. (2022). Compound droughts and hot extremes: Characteristics, drivers, changes, and impacts. *Earth-Science Reviews*, 235(19), 104241. <https://doi.org/10.1016/j.earscirev.2022.104241>
- Harpenslager, S. F., van den Elzen, E., Kox, M. A., Smolders, A. J., Ettwig, K. F., & Lamers, L. P. (2015). Rewetting former agricultural peatlands: Topsoil removal as a prerequisite to avoid strong nutrient and greenhouse gas emissions. *Ecological Engineering*, 84, 159–168. <https://doi.org/10.1016/j.ecoleng.2015.08.002>
- Harrison, P. A., Vandewalle, M., Sykes, M. T., Berry, P. M., Bugter, R., de Bello, F., et al. (2010). Identifying and prioritising services in European terrestrial and freshwater ecosystems. *Biodiversity & Conservation*, 19(10), 2791–2821. <https://doi.org/10.1007/s10531-010-9789-x>
- Horton, D. E., Johnson, N. C., Singh, D., Swain, D. L., Rajaratnam, B., & Diffenbaugh, N. S. (2015). Contribution of changes in atmospheric circulation patterns to extreme temperature trends. *Nature*, 522(7557), 465–469. <https://doi.org/10.1038/nature14550>
- Intergovernmental Panel on Climate Change (IPCC). (2023). Weather and climate extreme events in a changing climate. In V. Masson-Delmotte (Ed.), et al. (Eds.), *Climate change 2021 – the physical science basis* (pp. 1513–1766). Cambridge University Press. <https://doi.org/10.1017/9781009157896.013>
- Jensen, K., & McDonald, K. (2019). Surface water microwave product series version 3: A near-real time and 25-year historical global inundated area fraction time series from active and passive microwave remote sensing. *IEEE Geoscience and Remote Sensing Letters*, 16(9), 1402–1406. <https://doi.org/10.1109/lgrs.2019.2898779>
- Jones, D. L., Hodge, A., & Kuzyakov, Y. (2004). Plant and mycorrhizal regulation of rhizodeposition. *New Phytologist*, 163(3), 459–480. <https://doi.org/10.1111/j.1469-8137.2004.01130.x>
- Kang, X., Yan, L., Cui, L., Zhang, X., Hao, Y., Wu, H., et al. (2018). Reduced carbon dioxide sink and methane source under extreme drought condition in an alpine peatland. *Sustainability*, 10(11), 1–15. <https://doi.org/10.3390/su10114285>
- Knorr, K. H., & Blodau, C. (2009). Impact of experimental drought and rewetting on redox transformations and methanogenesis in mesocosms of a northern fen soil. *Soil Biology and Biochemistry*, 41(6), 1187–1198. <https://doi.org/10.1016/j.soilbio.2009.02.030>



- Knox, S. H., Bansal, S., McNicol, G., Schafer, K., Sturtevant, C., Ueyama, M., et al. (2021). Identifying dominant environmental predictors of freshwater wetland methane fluxes across diurnal to seasonal time scales. *Global Change Biology*, 27(15), 3582–3604. <https://doi.org/10.1111/gcb.15661>
- Knox, S. H., Jackson, R. B., Poulter, B., McNicol, G., Fluet-Chouinard, E., Zhang, Z., et al. (2019). FluXNET-CH<sub>4</sub> synthesis activity objectives, observations, and future directions. *Bulletin of the American Meteorological Society*, 100(12), 2607–2632. <https://doi.org/10.1175/BAMS-D-18-0268.1>
- Kosten, S., van den Berg, S., Mendonça, R., Paranaíba, J. R., Roland, F., Sobek, S., et al. (2018). Extreme drought boosts CO<sub>2</sub> and CH<sub>4</sub> emissions from reservoir drawdown areas. *Inland Waters*, 8(3), 329–340. <https://doi.org/10.1080/20442041.2018.1483126>
- Lal, P., Shekhar, A., Gharun, M., & Das, N. N. (2023). Spatiotemporal evolution of global long-term patterns of soil moisture. *Science of the Total Environment*, 867(December 2022), 161470. <https://doi.org/10.1016/j.scitotenv.2023.161470>
- Leonard, M., Westra, S., Phatak, A., Lambert, M., van den Hurk, B., McInnes, K., et al. (2014). A compound event framework for understanding extreme impacts. *Wiley Interdisciplinary Reviews: Climate Change*, 5(1), 113–128. <https://doi.org/10.1002/wcc.252>
- Li, J., Pei, J., Fang, C., Li, B., & Nie, M. (2023). Opposing seasonal temperature dependencies of CO<sub>2</sub> and CH<sub>4</sub> emissions from wetlands. *Global Change Biology*, 29(4), 1133–1143. <https://doi.org/10.1111/gcb.16528>
- Long, K. D., Flanagan, L. B., & Cai, T. (2010). Diurnal and seasonal variation in methane emissions in a northern Canadian peatland measured by eddy covariance. *Global Change Biology*, 16(9), 2420–2435. <https://doi.org/10.1111/j.1365-2486.2009.02083.x>
- Malone, S. L., Starr, G., Staudhammer, C. L., & Ryan, M. G. (2013). Effects of simulated drought on the carbon balance of Everglades short-hydroperiod marsh. *Global Change Biology*, 19(8), 2511–2523. <https://doi.org/10.1111/gcb.12211>
- Moore, T. R., & Roulet, N. T. (1993). Methane flux: Water table relations in northern wetlands. *Geophysical Research Letters*, 20(7), 587–590. <https://doi.org/10.1029/93gl00208>
- Muñoz-Sabater, J., Dutra, E., Agustí-Panareda, A., Albergel, C., Arduini, G., Balsamo, G., et al. (2021). ERA5-Land: A state-of-the-art global reanalysis dataset for land applications. *Earth System Science Data*, 13(9), 4349–4383. <https://doi.org/10.5194/essd-13-4349-2021>
- Nazaries, L., Murrell, J. C., Millard, P., Baggs, L., & Singh, B. K. (2013). Methane, microbes and models: Fundamental understanding of the soil methane cycle for future predictions. *Environmental Microbiology*, 15(9), 2395–2417. <https://doi.org/10.1111/1462-2920.12149>
- Nisbet, E. G., Manning, M. R., Dlugokencky, E. J., Michel, S. E., Lan, X., Röckmann, T., et al. (2023). Atmospheric methane: Comparison between methane's record in 2006–2022 and during glacial terminations. *Global Biogeochemical Cycles*, 37(8). <https://doi.org/10.1029/2023GB007875>
- Novick, K. A., Biederman, J. A., Desai, A. R., Litvak, M. E., Moore, D. J., Scott, R. L., & Torn, M. S. (2018). The AmeriFlux network: A coalition of the willing. *Agricultural and Forest Meteorology*, 249, 444–456. <https://doi.org/10.1016/j.agrformet.2017.10.009>
- Olefeldt, D., Euskirchen, E. S., Harden, J., Kane, E., McGuire, A. D., Waldrop, M. P., & Turetsky, M. R. (2017). A decade of boreal rich fen greenhouse gas fluxes in response to natural and experimental water table variability. *Global Change Biology*, 23(6), 2428–2440. <https://doi.org/10.1111/gcb.13612>
- Olefeldt, D., Roulet, N. T., Bergeron, O., Crill, P., Bäckstrand, K., & Christensen, T. R. (2012). Net carbon accumulation of a high-latitude permafrost tundra mire similar to permafrost-free peatlands. *Geophysical Research Letters*, 39(3). <https://doi.org/10.1029/2011GL050355>
- Olefeldt, D., Turetsky, M. R., Crill, P. M., & McGuire, A. D. (2013). Environmental and physical controls on northern terrestrial methane emissions across permafrost zones. *Global Change Biology*, 19(2), 589–603. <https://doi.org/10.1111/gcb.12071>
- Parmentier, F. J. W., Rasse, D. P., Lund, M., Bjerke, J. W., Drake, B. G., Weldon, S., et al. (2018). Vulnerability and resilience of the carbon exchange of a subarctic peatland to an extreme winter event. *Environmental Research Letters*, 13(6), 065009. <https://doi.org/10.1088/1748-9326/aabff3>
- Peng, S., Lin, X., Thompson, R. L., Xi, Y., Liu, G., Hauglustaine, D., et al. (2022). Wetland emission and atmospheric sink changes explain methane growth in 2020. *Nature*, 612(7940), 477–482. <https://doi.org/10.1038/s41586-022-05447-w>
- Pirk, N., Santos, T., Gustafson, C., Johansson, A. J., Tuvesson, F., Parmentier, F. J. W., et al. (2015). Methane emission bursts from permafrost environments during autumn freeze-in: New insights from ground-penetrating radar. *Geophysical Research Letters*, 42(16), 6732–6738. <https://doi.org/10.1002/2015GL065034>
- Reiche, M., Hädrich, A., Lischeid, G., & Küsel, K. (2009). Impact of manipulated drought and heavy rainfall events on peat mineralization processes and source-sink functions of an acidic fen. *Journal of Geophysical Research*, 114(2), 1–13. <https://doi.org/10.1029/2008JG000853>
- Reichstein, M., Bahn, M., Ciais, P., Frank, D., Mahecha, M. D., Seneviratne, S. I., et al. (2013). Climate extremes and the carbon cycle. *Nature*, 500(7462), 287–295. <https://doi.org/10.1038/nature12350>
- Renom, M., Rusticucci, M., & Barreiro, M. (2011). Multidecadal changes in the relationship between extreme temperature events in Uruguay and the general atmospheric circulation. *Climate Dynamics*, 37(11–12), 2471–2480. <https://doi.org/10.1007/s00382-010-0986-9>
- Rinne, J., Tuovinen, J. P., Klemetsson, L., Aurela, M., Holst, J., Lohila, A., et al. (2020). Effect of the 2018 European drought on methane and carbon dioxide exchange of northern mire ecosystems: 2018 drought on northern mires. *Philosophical Transactions of the Royal Society B: Biological Sciences*, 375(1810), 20190517. <https://doi.org/10.1098/rstb.2019.0517>
- Ruehr, N. K., Grote, R., Mayr, S., & Arneith, A. (2019). Beyond the extreme: Recovery of carbon and water relations in woody plants following heat and drought stress. *Tree Physiology*, 39(8), 1285–1299. <https://doi.org/10.1093/treephys/tpz032>
- Saunio, M., Stavert, A. R., Poulter, B., Bousquet, P., Canadell, J. G., Jackson, R. B., et al. (2020). The Global Methane Budget 2000–2017. *Earth System Science Data*, 12(3), 1561–1623. <https://doi.org/10.5194/essd-12-1561-2020>
- Schamm, K., Ziese, M., Becker, A., Finger, P., Meyer-Christoffer, A., Schneider, U., et al. (2014). Global gridded precipitation over land: A description of the new GPCC first guess daily product. *Earth System Science Data*, 6(1), 49–60. <https://doi.org/10.5194/essd-6-49-2014>
- Schuur, E. A., McGuire, A. D., Schädel, C., Grosse, G., Harden, J. W., Hayes, D. J., et al. (2015). Climate change and the permafrost carbon feedback. *Nature*, 520(7546), 171–179. <https://doi.org/10.1038/nature14338>
- Schwalm, C. R., Williams, C. A., Schaefer, K., Arneith, A., Bonal, D., Buchmann, N., et al. (2010). Assimilation exceeds respiration sensitivity to drought: A FLUXNET synthesis. *Global Change Biology*, 16(2), 657–670. <https://doi.org/10.1111/j.1365-2486.2009.01991.x>
- Schwalm, C. R., Williams, C. A., Schaefer, K., Baldocchi, D., Black, T. A., Goldstein, A. H., et al. (2012). Reduction in carbon uptake during turn of the century drought in western North America. *Nature Geoscience*, 5(8), 551–556. <https://doi.org/10.1038/ngeo1529>
- Sen, P. K. (1968). Estimates of the regression coefficient based on Kendall's Tau. *Journal of the American Statistical Association*, 63(324), 1379–1389. <https://doi.org/10.1080/01621459.1968.10480934>
- Seneviratne, S. I., Lüthi, D., Litschi, M., & Schär, C. (2006). Land-atmosphere coupling and climate change in Europe. *Nature*, 443(7108), 205–209. <https://doi.org/10.1038/nature05095>
- Seneviratne, S. I., Nicholls, N., Easterling, D., Goodess, C. M., Kanae, S., Kossin, J., et al. (2012). Changes in climate extremes and their impacts on the natural physical environment. In *Managing the risks of extreme events and disasters to advance climate change adaptation* (pp. 109–230). <https://doi.org/10.1017/CBO9781139177245.006>



- Sturtevant, C., Ruddell, B. L., Knox, S. H., Verfaillie, J., Matthes, J. H., Oikawa, P. Y., & Baldocchi, D. (2016). Identifying scale-emergent, nonlinear, asynchronous processes of wetland methane exchange. *Journal of Geophysical Research: Biogeosciences*, 121(1), 188–204. <https://doi.org/10.1002/2015JG003054>
- Treat, C. C., Bloom, A. A., & Marushchak, M. E. (2018). Nongrowing season methane emissions—a significant component of annual emissions across northern ecosystems. *Global Change Biology*, 24(8), 3331–3343. <https://doi.org/10.1111/gcb.14137>
- Turetsky, M. R., Kotowska, A., Bubier, J., Dise, N. B., Crill, P., Hornibrook, E. R., et al. (2014). A synthesis of methane emissions from 71 northern, temperate, and subtropical wetlands. *Global Change Biology*, 20(7), 2183–2197. <https://doi.org/10.1111/gcb.12580>
- Turetsky, M. R., Treat, C. C., Waldrop, M. P., Waddington, J. M., Harden, J. W., & McGuire, A. D. (2008). Short-term response of methane fluxes and methanogen activity to water table and soil warming manipulations in an Alaskan peatland. *Journal of Geophysical Research*, 113(3). <https://doi.org/10.1029/2007JG000496>
- van den Berg, M., van den Elzen, E., Ingwersen, J., Kosten, S., Lamers, L. P., & Streck, T. (2020). Contribution of plant-induced pressurized flow to CH<sub>4</sub> emission from a Phragmites fen. *Scientific Reports*, 10(1), 12304. <https://doi.org/10.1038/s41598-020-69034-7>
- Voigt, C., Lamprecht, R. E., Marushchak, M. E., Lind, S. E., Novakovskiy, A., Aurela, M., et al. (2017). Warming of subarctic tundra increases emissions of all three important greenhouse gases – Carbon dioxide, methane, and nitrous oxide. *Global Change Biology*, 23(8), 3121–3138. <https://doi.org/10.1111/gcb.13563>
- Von Buttlar, J., Zscheischler, J., Rammig, A., Sippel, S., Reichstein, M., Knohl, A., et al. (2018). Impacts of droughts and extreme-temperature events on gross primary production and ecosystem respiration: A systematic assessment across ecosystems and climate zones. *Biogeosciences*, 15(5), 1293–1318. <https://doi.org/10.5194/bg-15-1293-2018>
- Vroom, R. J., van den Berg, M., Pangala, S. R., van der Scheer, O. E., & Sorrell, B. K. (2022). Physiological processes affecting methane transport by wetland vegetation – a review. *Aquatic Botany*, 182(July), 103547. <https://doi.org/10.1016/j.aquabot.2022.103547>
- Wolf, S., Keenan, T. F., Fisher, J. B., Baldocchi, D. D., Desai, A. R., Richardson, A. D., et al. (2016). Warm spring reduced carbon cycle impact of the 2012 US summer drought. *Proceedings of the National Academy of Sciences of the United States of America*, 113(21), 5880–5885. <https://doi.org/10.1073/pnas.1519620113>
- Xu, M., Zhang, J., Zhang, Z., Wang, M., Chen, H., Peng, C., et al. (2024). Global responses of wetland methane emissions to extreme temperature and precipitation. *Environmental Research*, 252(P3), 118907. <https://doi.org/10.1016/j.envres.2024.118907>
- Yuan, J., Liu, D., Ji, Y., Xiang, J., Lin, Y., Wu, M., & Ding, W. (2019). *Spartina alterniflora* invasion drastically increases methane production potential by shifting methanogenesis from hydrogenotrophic to methylotrophic pathway in a coastal marsh. *Journal of Ecology*, 107(5), 2436–2450. <https://doi.org/10.1111/1365-2745.13164>
- Zhang, Z., Poulter, B., Feldman, A. F., Ying, Q., Ciais, P., Peng, S., & Li, X. (2023). Recent intensification of wetland methane feedback. *Nature Climate Change*, 13(5), 430–433. <https://doi.org/10.1038/s41558-023-01629-0>
- Zhang, Z., Zimmermann, N. E., Stenke, A., Li, X., Hodson, E. L., Zhu, G., et al. (2017). Emerging role of wetland methane emissions in driving 21st century climate change. *Proceedings of the National Academy of Sciences of the United States of America*, 114(36), 9647–9652. <https://doi.org/10.1073/pnas.1618765114>
- Zhao, J., Peichl, M., & Nilsson, M. B. (2016). Enhanced winter soil frost reduces methane emission during the subsequent growing season in a boreal peatland. *Global Change Biology*, 22(2), 750–762. <https://doi.org/10.1111/gcb.13119>
- Zhuang, Q., Zhu, X., He, Y., Prigent, C., Melillo, J. M., David McGuire, A., et al. (2015). Influence of changes in wetland inundation extent on net fluxes of carbon dioxide and methane in northern high latitudes from 1993 to 2004. *Environmental Research Letters*, 10(9), 095009. <https://doi.org/10.1088/1748-9326/10/9/095009>
- Ziese, M., Rauthe-Schöch, A., Becker, A., Finger, P., Meyer-Christoffer, A., & Schneider, U. (2018). *GPCC full data daily Version.2018 at 1.0 degree: Daily land-surface precipitation from rain-gauges built on GTS-based and historic data*. Global Precipitation Climatology Centre. [https://doi.org/10.5676/DWD\\_GPCC/FD\\_D\\_V2022\\_100](https://doi.org/10.5676/DWD_GPCC/FD_D_V2022_100)
- Zou, J., Ziegler, A. D., Chen, D., McNicol, G., Ciais, P., Jiang, X., et al. (2022). Rewetting global wetlands effectively reduces major greenhouse gas emissions. *Nature Geoscience*, 15(8), 627–632. <https://doi.org/10.1038/s41561-022-00989-0>
- Zscheischler, J., Mahecha, M. D., Harmeling, S., & Reichstein, M. (2013). Detection and attribution of large spatiotemporal extreme events in Earth observation data. *Ecological Informatics*, 15, 66–73. <https://doi.org/10.1016/j.ecoinf.2013.03.004>
- Zscheischler, J., Reichstein, M., Harmeling, S., Rammig, A., Tomelleri, E., & Mahecha, M. D. (2014). Extreme events in gross primary production: A characterization across continents. *Biogeosciences*, 11(11), 2909–2924. <https://doi.org/10.5194/bg-11-2909-2014>

## References From the Supporting Information

- Bergamaschi, B., & Windham-Myers, L. (2018). *AmeriFlux AmeriFlux US-SrrSuisun marsh - rush ranch*. AmeriFlux; United States Geological Survey; USGS. <https://doi.org/10.17190/AMF/1418685>
- Billesbach, D., & Sullivan, R. (2019). *AmeriFlux AmeriFlux US-A10 ARM-NSA-barrow*. AmeriFlux; Argonne National Laboratory. <https://doi.org/10.17190/AMF/1498753>
- Billesbach, D., & Sullivan, R. (2020). *FLUXNET-CH<sub>4</sub> US-A03 ARM-AMF3-Olitok*. FluxNet; Argonne National Laboratory. <https://doi.org/10.18140/FLX/1669661>
- Bohrer, G. (2016). *AmeriFlux AmeriFlux US-ORv olentangy river wetland research park*. AmeriFlux; The Ohio State University. <https://doi.org/10.17190/AMF/1246135>
- Campbell, D., & Goodrich, J. (2020). *FLUXNET-CH<sub>4</sub> NZ-Kop kopuatai*. FluxNet; University of Waikato. <https://doi.org/10.18140/FLX/1669652>
- Chamberlain, S., Oikawa, P., Sturtevant, C., Szutu, D., Verfaillie, J., & Baldocchi, D. (2016). *AmeriFlux AmeriFlux US-tw3 Twitchell Alfalfa*. AmeriFlux; University of California. <https://doi.org/10.17190/AMF/1246149>
- Christen, A., & Knox, S. (2019). *AmeriFlux AmeriFlux CA-DBB Delta Burns bog*. AmeriFlux; University of British Columbia. <https://doi.org/10.17190/AMF/1543378>
- Desai, A. R. (2016a). *AmeriFlux AmeriFlux US-Los lost Creek*. AmeriFlux; University of Wisconsin. <https://doi.org/10.17190/AMF/1246071>
- Desai, A. R. (2016b). *AmeriFlux AmeriFlux US-PFa Park Falls/WLEF*. AmeriFlux; University of Wisconsin. <https://doi.org/10.17190/AMF/1246090>
- Detto, M., Sturtevant, C., Oikawa, P., Verfaillie, J., & Baldocchi, D. (2020). *FLUXNET-CH<sub>4</sub> US-Snd Sherman Island*. FluxNet; University of California. <https://doi.org/10.18140/FLX/1669692>
- Dolman, H., Maximov, T., Parmentier, F., & Budishev, A. (2020). *FLUXNET-CH<sub>4</sub> RU-Cok Chokurdakh*. FluxNet; Vrije Universiteit Amsterdam. <https://doi.org/10.18140/FLX/1669656>

- Eichmann, E., Shortt, R., Knox, S. H., Sanchez, C., Valach, A., Sturtevant, C., et al. (2016). *AmeriFlux AmeriFlux US-Tw4 Twitchell East end wetland*. AmeriFlux; University of California. <https://doi.org/10.17190/AMF/1246151>
- Euskirchen, E. (2021). *AmeriFlux AmeriFlux US-BZF Bonanza Creek rich fen*. AmeriFlux; University of Alaska Fairbanks, Institute of Arctic Biology. <https://doi.org/10.17190/AMF/1756433>
- Euskirchen, E. (2022). *AmeriFlux FLUXNET-1F US-BZB Bonanza Creek Thermokarst bog*. AmeriFlux; University of Alaska Fairbanks, Institute of Arctic Biology. <https://doi.org/10.17190/AMF/1881569>
- Euskirchen, E., Shaver, G., & Bret-Harte, S. (2016). *AmeriFlux AmeriFlux USICs Innvait Creek Watershed wet sedge tundra*. AmeriFlux; Marine Biological Laboratory; University of Alaska Fairbanks. <https://doi.org/10.17190/AMF/1246130>
- Hinkle, C. (2019). *AmeriFlux AmeriFlux US-DPW Disney Wilderness Preserve wetland*. AmeriFlux; University of Central Florida; University of Central Florida (UCF). <https://doi.org/10.17190/AMF/1562387>
- Knox, S. H., Matthes, J., Verfaillie, J., & Baldocchi, D. (2016). *AmeriFlux Ameri-flux US-Twt Twitchell Island*. AmeriFlux; University of California. <https://doi.org/10.17190/AMF/1246140>
- Koebisch, F., & Jurasinski, G. (2020). *FLUXNET-CH<sub>4</sub> DE-Hte Huetelmoor.FluxNet; Landscape Ecology*. University of Rostock. <https://doi.org/10.18140/FLX/1669634>
- Lohila, A., Aurela, M., Tuovinen, J.-P., Laurila, T., Hatakka, J., Ranne, J., & M'akela, T. (2020). *FLUXNET-CH<sub>4</sub> FI-Lom Lompolojankka*. FluxNet; Finnish Meteorological Institute. <https://doi.org/10.18140/FLX/1669638>
- Matthes, J., Sturtevant, C., Oikawa, P., Chamberlain, S., Szutu, D., Arias-Ortiz, A., et al. (2016). *AmeriFlux AmeriFlux US-Myb Mayberry wetland*. AmeriFlux; University of California. <https://doi.org/10.17190/AMF/1246139>
- Merbold, L., Fuchs, K., Buchmann, N., & Ho'rtanag, L. (2020). *FLUXNET-CH<sub>4</sub> CHCha Chamau*. FluxNet; ETH Zurich. <https://doi.org/10.18140/FLX/1669629>
- Nilsson, M., & Peichl, M. (2020). *FLUXNET-CH<sub>4</sub> SE-Deg Degero*. FluxNet; Department of Forest Ecology and Management; Swedish University of Agricultural Sciences. <https://doi.org/10.18140/FLX/1669659>
- Noormets, A. (2022). *AmeriFlux FLUXNET-1F US-NC4 NC AlligatorRiver*. Amer-iFlux; Texas A and M University. <https://doi.org/10.17190/AMF/1902837>
- Rey-Sanchez, C., Wang, C., Szutu, D., Hemes, K., Verfaillie, J., & Baldocchi, D. (2018). *AmeriFlux AmeriFlux US-Bi2 Bouldin Island corn*. AmeriFlux; University of California. <https://doi.org/10.17190/AMF/1419513>
- Rey-Sanchez, C., Wang, C., Szutu, D., Shortt, R., Chamberlain, S., Verfaillie, J., & Baldocchi, D. (2022). *AmeriFlux FLUXNET-1F US-Bi1 Bouldin Island Al-falfa*. AmeriFlux; University of California. <https://doi.org/10.17190/AMF/1871134>
- Richardson, A., & Hollinger, D. (2020). *FLUXNET-CH<sub>4</sub> US-Ho1 Howland Forest (main tower)*. FluxNet; USDA Forest Service. <https://doi.org/10.18140/FLX/1669675>
- Roman, T., Kolka, R., Griffis, T., & Deventer, J. (2021). *AmeriFlux AmeriFlux US-MBP Marcell bog lake peatland*. AmeriFlux; University of Minnesota; USDA- Forest Service. <https://doi.org/10.17190/AMF/1767835>
- Ryu, Y., Kang, M., & Kim, J. (2020). *FLUXNET-CH<sub>4</sub> KR-CRK Cheorwon rice paddy*. FluxNet; National Center for AgroMeteorology; Seoul National University. <https://doi.org/10.18140/FLX/1669649>
- Sachs, T., & Wille, C. (2020a). *FLUXNET-CH<sub>4</sub> DE-Dgw Dagowsee*. FluxNet; GFZ German Research Centre for Geosciences. <https://doi.org/10.18140/FLX/1669633>
- Sachs, T., & Wille, C. (2020b). *FLUXNET-CH<sub>4</sub> DE-Zrk Zamekow*. FluxNet; GFZ German Research Centre for Geosciences. <https://doi.org/10.18140/FLX/1669636>
- Schuur, T. (2018). *AmeriFlux AmeriFlux US-EML Eight mile lake permafrost thaw gradient, healy Alaska*. AmeriFlux; Northern Arizona University; University of Northern Arizona. <https://doi.org/10.17190/AMF/1418678>
- Shortt, R., Hemes, K., Szutu, D., Verfaillie, J., & Baldocchi, D. (2018). *AmeriFlux AmeriFlux US-Sne Sherman Island Restored wetland*. AmeriFlux; University of California. <https://doi.org/10.17190/AMF/1418684>
- Sonnentag, O., & Helbig, M. (2020). *FLUXNET-CH<sub>4</sub> CA-SCC Scotty Creek land scape*. FluxNet; Universit'e de Montr'eal; Wilfrid Laurier University. <https://doi.org/10.18140/FLX/1669628>
- Sonnentag, O., & Quinton, W. (2019). *AmeriFlux AmeriFlux CA-SCB Scotty Creek bog*. AmeriFlux; Universit'e de Montr'eal; Wilfrid Laurier University. <https://doi.org/10.17190/AMF/1498754>
- Torn, M., & Dengel, S. (2020a). *AmeriFlux AmeriFlux US-NGC NGEE Arctic Council*. AmeriFlux; Berkeley Lab; Lawrence Berkeley National Laboratory. <https://doi.org/10.17190/AMF/1634883>
- Torn, M., & Dengel, S. (2020b). *FLUXNET-CH<sub>4</sub> US-NGB NGEE Arctic Barrow*. FluxNet; Lawrence Berkeley National Laboratory. <https://doi.org/10.18140/FLX/1669687>
- Ueyama, M., Hirano, T., & Kominami, Y. (2020). *FLUXNET-CH<sub>4</sub> JP-BBY Bibai bog*. FluxNet; Osaka Prefecture Univeristy. <https://doi.org/10.18140/FLX/1669646>
- Ueyama, M., Iwata, H., & Harazono, Y. (2018). *AmeriFlux AmeriFlux US-Uaf University of Alaska, Fairbanks*. AmeriFlux; Osaka Prefecture University; Shinshu University. <https://doi.org/10.17190/AMF/1480322>
- Valach, A., Shortt, R., Szutu, D., Eichmann, E., Knox, S. H., Hemes, K., et al. (2016). *AmeriFlux AmeriFlux US-Tw1 Twitchell wetland west Pond*. AmeriFlux; University of California. <https://doi.org/10.17190/AMF/1246147>
- Vargas, R. (2018). *AmeriFlux AmeriFlux US-StJ st Jones Reserve*. AmeriFlux; University of Delaware. <https://doi.org/10.17190/AMF/1480316>
- Varlagin, A. (2020). *FLUXNET-CH<sub>4</sub> RU-Fy2 Fyodorovskoye dry spruce*. FluxNet; A.N. Severtsov Institute of Ecology and Evolution RAS. <https://doi.org/10.18140/FLX/1669657>
- Vesala, T., Tuittila, E.-S., Mammarella, I., & Alekseychik, P. (2020a). *Fluxnet ch4 fi-si2 siikaneva-2 bog*. FluxNet; University of Eastern Finland; University of Helsinki. <https://doi.org/10.18140/FLX/1669639>
- Vesala, T., Tuittila, E.-S., Mammarella, I., & Alekseychik, P. (2020b). *FLUXNET CH<sub>4</sub> FI-Sii siikaneva*. FluxNet; University of Eastern Finland; University of Helsinki. <https://doi.org/10.18140/FLX/1669640>
- Vourlitis, G., Dalmagro, H., De, S., Nogueira, J., Johnson, M., & Arruda, P. (2019). *AmeriFlux AmeriFlux BR-Npw northern Pantanal wetland*. AmeriFlux; California State University, San Marcos; Universidade de Cuiaba; Universidade Federal de Mato Grosso; University of British Columbia. <https://doi.org/10.17190/AMF/1579716>
- Zona, D., & Oechel, W. (2016). *AmeriFlux AmeriFlux US-Ivo Ivotuk*. Ameri-Flux; San Diego State University. <https://doi.org/10.17190/AMF/1246067>
- Zona, D., & Oechel, W. (2020). *FLUXNET-CH<sub>4</sub> US-Atq Atqasuk*. FluxNet; San Diego State University. <https://doi.org/10.18140/FLX/1669663>